Host University: The University of Edinburgh – The University of Queensland

Faculty: School of Engineering – The Faculty of Engineering, Architecture and Information Technology

Department: Institute of Infrastructure and Environment – School of Civil Engineering

Academic Year 2018-2020

RESPONSE OF TALL BUILDING DIAGRID STRUCTURE TO INTERMEDIATE AND MEGA FLOOR FIRE

Waqas Haider

Promoter(s): Dr. Angus Law, Dr. David Lange

Master thesis submitted in the Erasmus+ Study Programme

International Master of Science in Fire Safety Engineering

Table of Contents

DISCLAIMER

This thesis is submitted in partial fulfilment of the requirements for the degree of *The International Master of Science in Fire Safety Engineering (IMFSE)*. This thesis has never been submitted for any degree or examination to any other University/programme. The author(s) declare(s) that this thesis is original work except where stated. This declaration constitutes an assertion that full and accurate references and citations have been included for all material, directly included and indirectly contributing to the thesis. The author(s) gives (give) permission to make this master thesis available for consultation and to copy parts of this master thesis for personal use. In the case of any other use, the limitations of the copyright have to be respected, in particular with regard to the obligation to state expressly the source when quoting results from this master thesis. The thesis supervisor must be informed when data or results are used.

Read and approved,

Waqas Haider

30-Apr-2020

Abstract

Response of tall building diagrid structure to intermediate and mega floor fire has been studied in this thesis. The analysis was performed for a 36-story building with steel diagrid structure. Four fire scenarios were developed: two for lower floors (i.e. floor 3 & 4) and two for upper floors (i.e. floor 33 & 34). Standard fir curve i.e. ISO-834 was used for this study. The results show that the failure mechanism is different for intermediate and mega floor fire scenario on lower floors in a tall building. In case of intermediate floor fire, failure was initiated due to the buckling of diagrid at the base while in mega floor fire, failure was initiated due to plastic hinge formation in the floor beam. In case of fire on upper floors in the building, failure was indicated by large deflections in the slab.

Development of deflections, axial forces and bending moments were also analyzed. Results show that the largest compressive stresses develop in the fire floor. The floors adjacent to the fire floor experience highest tensile forces. Theses tensile forces reduce as we move to the floors away from the fire floor. The diagrid lateral displacement depends on the relative stiffness of floor beams and diagrid section. The lateral displacement of diagrid, inwards and outwards, is higher in case of mega floor fire.

Declaration of Covid-19 Impact

a) Impact on studies

I always had a hard time to study in my room and I usually stayed late in the campus or went to library to stay focused and productive. I came to The University of Queensland for my thesis and was allotted a desk with a computer and a laptop to work on campus. The main task for the thesis was computer modelling and simulations. It was very helpful for me to come to the university and have a regular routine. Every evening I had a sense of accomplishment that I had a productive day.

In the 2nd week of March, the UQ advised to work from home if possible. Though it was not mandatory but I did not want to neglect the advice. On 17th of March, we were asked to stop the numerical work by The University of Edinburgh.

Most of the time during practical work was invested in understanding the tool-which was new for me. It took a lot of time to understand the modelling techniques, fixing all the errors and running of the 1st 3D model. This was the most challenging and demanding milestone to achieve. For the new models, it was mainly changing of some geometry and creating fire scenarios. Unfortunately, due to the unusual circumstances, work was stopped and simulations could not be completed. Following flowchart shows the initial plan of 16 scenarios, while I could complete only four of them, highlighted in grey.

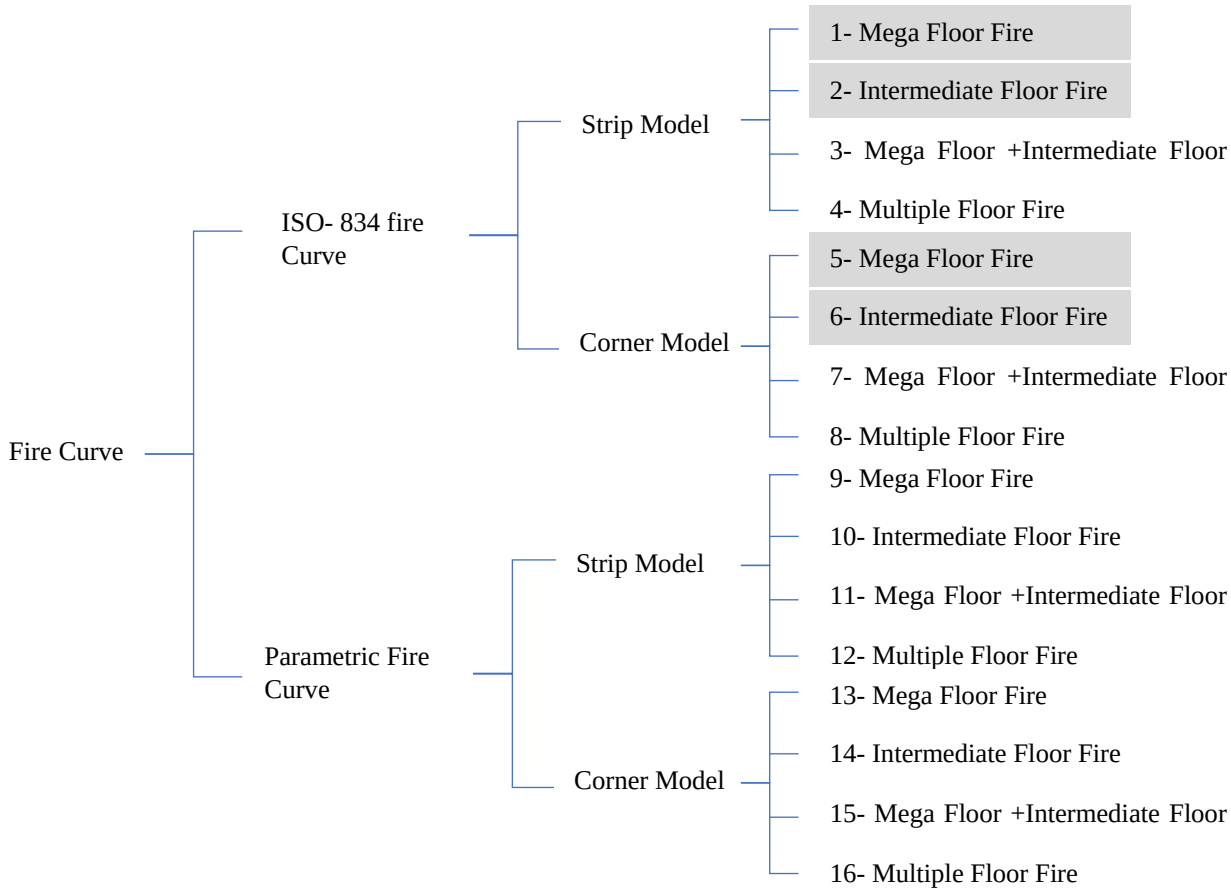

Besides this, after the initial run of 1st four models, I was planning to change a boundary condition, this is further explained in report Section 2.3.4 a), and see the difference in output. Which eventually could not be completed.

I started working from home by analyzing the results that I had and writing the thesis. Though I still had enough time to go in detailed literature review and interpret the results that I had, but it was really hard to stay focused. Hardly had I managed to allocate regular time to studies yet productivity was affected because of a lot of factors. Even after hours of work I would realize that I had not progressed much. I couldn't write up all the literature extract that I studied for the modelling and analysis of the results.

b) Impact on personal life

During infancy of the virus, it became difficult to focus on work. All the news, emails and discussions about the virus started stress and lack of focus. But I had the hardest time when cases stared to rise in my home country. On the one hand I was worried for my family and on the other hand I wanted to stay safe to work on my thesis. There was also a fear of getting sick with noxious infection being away from home. The conditions affected my productivity adversely. Though I could not complete the thesis to the level I had planned but still all the support from the supervisor, peers, management and the university, helped a lot to complete the thesis.

School of Engineering – Incident Management

Project Status Declaration

This form is to be used in unforeseen circumstances necessitating the immediate cessation of practical project work during semester. It acts as a record of the current status of practical work (whether it be laboratory based, computational, or fieldwork). Due to circumstances, ***no further practical work is to be continued, regardless of the type of work or current status***. This ensures equality of opportunity for all students, regardless of the type of work being undertaken.

The form must be completed during a meeting with the student, and verified by the student, supervisor, and either the thesis examiner, or a second supervisor. **Any practical work beyond that stated in this form will not be considered in the final project assessment.**

A copy of the signed form must be included in the final project submission.

Name: **Waqas Haider**_____ Student number: **S2005756** _____

Work completed

All items of wholly, or partially completed work must be listed, indicating the percentage completion for each task. Reference can be made to an attached project plan if appropriate. **Please take care to provide a full detailed list of all work done.**

My task was to prepare 3D structural model of a diagrid structure, using finite element tool (SAFIR) and study its mechanical response to fire. I followed the diagrid design by Jani & Patel, 2013 [1]. For this purpose, I prepared two kind of partial models of the structure. Building floor plan is 36m x 36m and is 36 storeys high. Both the models are for 6 floors in height while have different floor areas. The loads of upper 30 floors have been applied as nodal loads.

1. Model 1
   This is modelling of one third of the floor area. Floor plan is divided from Grid 1-4 & A-D and I modelled it between Grid 2-3 & A-D.
2. Model 2
   This is modelling of one quarter of the floor area in one corner of the floor plan.

Firstly, I completed the 2D thermal analysis of all structural element sections under ISO-834 fire. Then I used these section in 3D modelling of Model 1 and 2 mentioned above. For each model I completed two fire scenarios of ISO fire, one for fire on a mega floor and one on intermediate floor. So, in total I have four 3D structural model simulation results.

Work not commenced

Any items of outstanding work that have not been started should be listed here.

I was planning to run four sub-models of each of two models, mentioned previously, under ISO fire and four under parametric fire considering cooling phase. So, in total of 16 3D structural models, eight for Model-1 and eight for Model-2. Hence, I couldn't complete four structural models under ISO fire and all of eight under parametric fire.

Plans for completing project submission

State revised plans for producing the final project submission in the absence of any additional practical work beyond that already listed. For example, this may include literature-based research, or more in-depth analysis of results already obtained. Dates for completion of each element should be given.

I would say, in particularly it doesn't change much off my plan because I already have some of the major simulation results which I had planned. Though I was planning to run more fire scenarios which could be helpful to predict precisely the failure mode of diagrid but still the scope of work remains the same with fewer simulation results. I will complete the model validation by the end of March and then results and discussion will continue along with thesis writing until end of April.

Declaration

To the best of our knowledge, this form is an accurate record of the project status and revised completion plans on **30th of April 2020** _ (date)

Student:  _____ (Signature)

Supervisor:  _____

Second sup./Thesis examiner:  _____

[1] *Jani, K., & Patel, P. (2013). Analysis and Design of Diagrid Structural System for High Rise Steel Buildings. Procedia Engineering, 51, 92-100*

1. Introduction & Objective:

The growth in population, especially in the metropolitan areas created the need of vertical development. This gave rise to modern skyscrapers. With the innovation there comes the challenges. As we increase the height of the building, lateral forces on the structure become more significant than the gravitational loads. Thus, lateral load resisting structures like rigid frame, shear wall, braced tube system and tubular system became more common. Engineers and architectures are motivated to find the solution of modern challenges which leads to innovative structural designs. One of the modern innovations to the high-rise buildings is the diagrid structure. This did not only fulfill the structural design criteria but also gave rise to some of the landmark modern buildings. This system is laterally stiff and vertically strong which does not rely completely on the internal core and vertical column system inside the building. Hence, there can be few columns to no columns inside the building and more flexible interior design can be achieved with more free space.

1.1. Brief History of Diagrid Structures

The diagonal arrangement of the structural members to achieve higher strength and stiffness is not new, but recently this arrangement in the form of diagrid in high rise buildings has become more common, especially in the case of curves shapes and complex geometries.

The world's first diagrid structure was The Shukhov tower in Moscow, it was an exposed lattice diagrid designed in 1896 by a Russian engineer, Vladimir Shukhov. The construction was carried out 1920-1922. This was 350 m high. [1]

One of the earlier examples of the diagrid structure building is the IBM building in Pittsburg, USA. This was built in early 1960s. This building was 13 story and 58m high. This was also steel structure diagrid [2].

With the advent of technology and innovation in building design, the use of diagrid structure has diversified in terms of building design and aesthetics. Some of the modern examples of the diagrid structure are Swiss Re tower in London, Hearst tower in New York, Mode Gakuen spiral tower in Aichi, CCTV headquarter building in Beijing, Zhongguo Zun tower in Beijing, Capital Gate Abu Dhabi and Lotte super tower in Seoul (under construction) etc.

1.2. Objective of Thesis

There has been a lot of research on collapse mechanism of tall buildings in case of fire but there is little research for the response of tall building diagrid structure to fire.

The objective of thesis is to study the structural response of tall building diagrid structure to fire on mega floor and intermediate floor. A finite element modelling (FEM) tool will be employed to carry out this research. The tool used for FE modeling is SAFIR. The diagrid design followed is work carried out by Jani et al. [3]

1.3. Literature Review

1.3.1. Configuration of Diagrid Structures

Diagrid systems are the evolution of tubular braced structures. The key difference between a braced tube building and a diagrid building is that in the periphery of the diagrid building there are no vertical columns present. These vertical columns are replaced by the inclined columns which form a triangular pattern.

Fig. 1 shows a typical arrangement of the diagrid structure [1]. The main components of the diagrid are as following:

- Node
- Diagonal members
- Ring Beams
- Floor beams

The diagonal members are connected in a triangular pattern with each other at the nodes at flor level. The nodes are connected to each other with ring beams. The peripheral beams at the floor level where diagonal members join, is called ring beam. While the peripheral beams at other floors are called floor beams. A pair of triangular configurations is called module of the diagrid which consists of the four diagonal member. There could be varying number of floors in a module. Various section types are used for the diagrid.

The angle of inclination of these diagonal members is very important in the structural performance of the diagrid. Lateral stiffness of the structure is controlled by changing this angle. Numerous studies have been done for the optimum module height with respect to building height and angle of inclination of diagonal members [4]. Moon et al. studied the diagonal angle in the range of 34^o to 82^o in 20 to 60-story buildings. They conclude that the most efficient angle for a 42-story building having an aspect ratio of 5, the diagrid angle for maximum lateral stiffness range from 55^o to 65^o while for a 60-story building, with an aspect ratio of 7, this angle ranges from 65^o to 75^o [5].

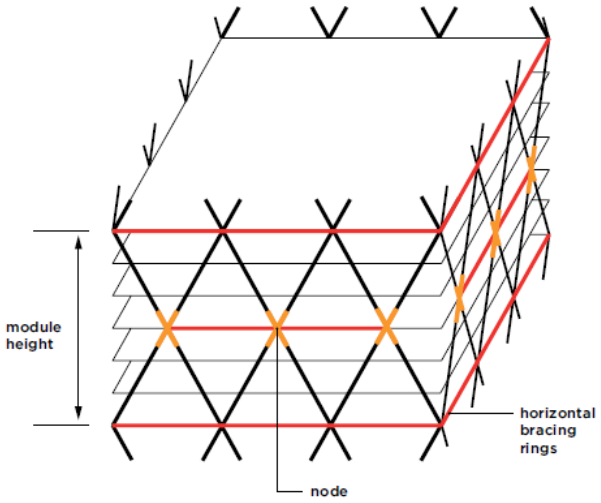

Fig. 1 A 3-story diagrid module and a triangular element [1]

1.3.2. Benefits of Diagrid Structures

The main idea for the development of the diagrid structure was the sustainability and saving by the removal of most of the vertical columns and thus engineer a configuration of the periphery of the building which would be able to support gravity as well as lateral loads.

The diagonal members in diagrid structures act both as inclined columns and as bracing elements, and mainly internal axial forces arise in the members due to their triangulated configuration. Diagrid structures do not need high shear rigidity cores because the diagrids located on the perimeter can carry shear. The number of columns inside the building is reduces significantly. Moreover, A diagrid system's design and efficiency decreases the number of structural elements required on the buildings' façade, thus less interference to the outside view. The corner beams can

Diagrid structures are more appealing aesthetically. They give the flexibility to complex building design. The diagrid structural system is also more sustainable, it can also save approximately 20% of the structural steel as compared to the moment-frame structure [1]. This may vary from project to project and the cost of engineering and fabrication may significantly be higher from the traditional buildings.

In some of the tall buildings like Burj Khalifa in Dubai, the size of the base of the building was increased to resist the moment. This can be avoided in the diagrid structures. Such as Swiss Re has even a narrow base and rely on the diagrid structure for the stability [1]

A number of different materials can be used for the construction of the diagrid but the most common material is steel. This can be used in conjunction with concrete.

1.3.3. Case Studies

1.3.3.1. Swiss Re tower

The Swiss Re Tower, which is also known as 30 Structure. Mary axe, is one of the modern diagrid structures. It was designed by the collaboration of Foster + Partners, Arup and RWDI. It is a perfect example of the criteria for a joint partnership solution involving architecture practice, engineering companies, and steel contractors as the basis for achieving a successful result when such a unique project is being taken.

Fig. 2 shows the mid-level plan of the building. It is a circular plan and the building’s diameter varies with height. It has 40 storeys and a central steel frame core. The perimeter diagrid structure is tubular steel sections and connects at the alternative floors with bolted connections at nodes. Thus, there are 4 floors in a module. The radial beam elements join core to the external diagrid structure. Fig. 3 shows the connection of the elements [1, p. 41]. The diagrid elements are straight but due to height of the building and smaller module height it seems all the way curve. The building has 90 minutes fire protection of the structural steel [1].

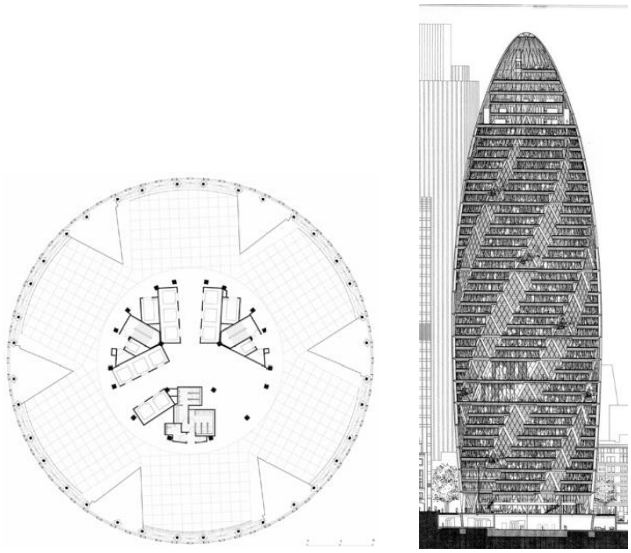

Fig. 2 Mid-level floor Plan [1, p. 39] *(left) and Illustrative section* [6] *(right) of Swiss Re tower*

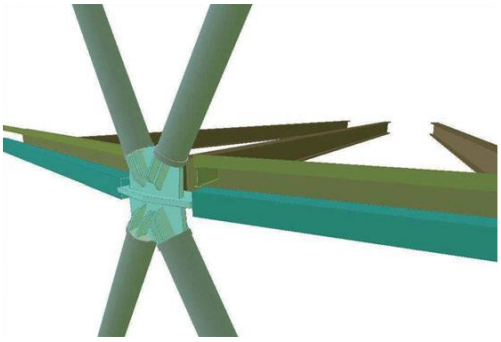

Fig. 3 Connection detail at Node [1, p. 41]

1.3.3.2. **Capital Gate**

The Capital Gate, Abu Dhabi was designed by RMJM. The diagrid members join at each floor. Hence, the building has one of the smallest diagrid modules with two floors tip to tip. The tower leans 18^{o} on one side. Fig. 5 shows the vertical section of the building in which inclination can be seen. This is one of the reasons to keep very small module height to accommodate the stresses due to this unique design. The stability is also supported by the presence of a concrete core. The size of the diagrid section and angle of inclination varies throughout the building and hence the design of node changes accordingly. However, the angle is generally around 45^{o} [1, p. 70]. The diagrid structure is the combination of interior and exterior diagrids, connected by the steel floor beams. The external diagrid defines the diagrid shape and internal diagrid is for the interior atrium. Interior atrium can be seen in the floor plan in Fig. 5 [1, p. 105].

Fig. 4 Vertical section of the building

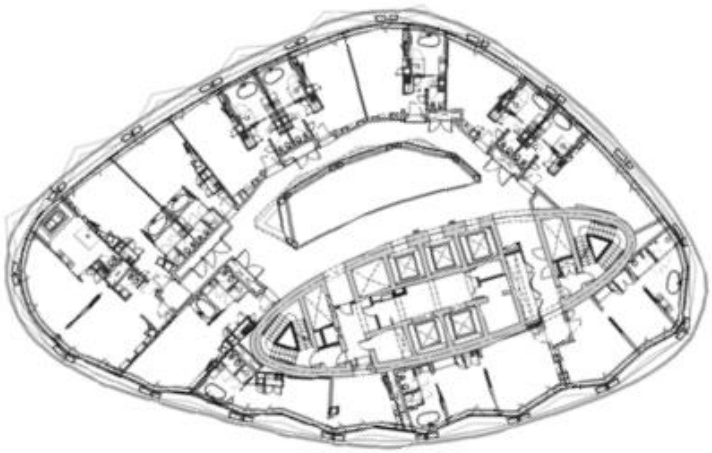

Fig. 5 Floor Plan at the section of atrium

1.3.3.3. **Hearst Tower**

The Hearst tower was designed by Foster and Partners with the collaboration with WSP Cantor Seinuk as the structural engineers. The building has a square foot print and the base of the tower sits in the existing historic building. The façade is supported by the steel columns and spandrel beams. The diagrid members are wide flange steel section and the nodes are made of welded plate sections. The diagrid members connect at each fourth floor and thus there are eight floors in one module. Hence, this is one of the large-scale diagrid module buildings.

There are no columns between exterior wall and core and the core is toward the backside of the building, this can be seen in Fig. 6 [1, p. 45]. The core is braced frame steel structure.

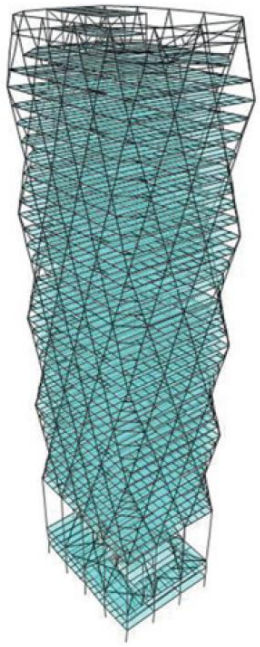

Fig. 6 Image of the steel structure, showing eccentricity of the core

1.3.4. Fire for structural design

1.3.4.1. Standard fire curve

Nowadays the standard fire curves are commonly used in order to unify the fire safety methods, both in the safety of construction materials and in the design of buildings for fire protection. In the Eurocode. Generally, two fire curves are stated as standard fire curve and can be used for different fire scenarios, Cellulosic Temperature-time fire curve and Hydrocarbon Temperature-time fire curve. However, Popular design methods for evaluating fire safety systems applied to structural steel components used in buildings are usually based on the standard cellulosic temperature-time curve [7].

The cellulosic standard fire curve follows the following fixed relation

$$\theta_g = \theta_{g,0} + 345 * log_{10}^{8t+1}$$

Where

$\theta_{g,0}$: initial gas temperature (20 ^{o}C)

θ_g: gas temperature (^{o}C) at the time t

t: time (min)

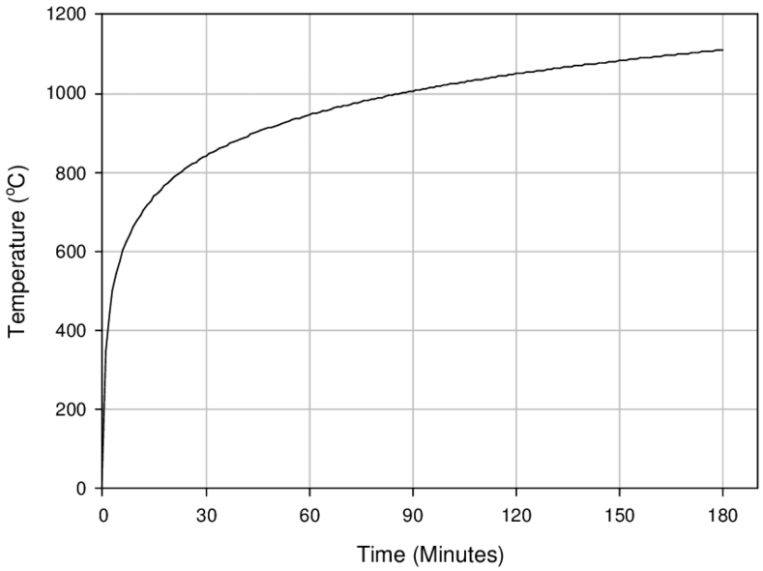

Fig. 7 ISO 834 fire curve

However, the standard fire curve does not reflect realistic fire exposure: it is fixed and the temperature always increases in time.

1.3.4.2. **Parametric fire curve**

The standard fire is independent of various parameters which may affect the actual fire intensity. This brings a number of new design possibilities including the parametric temperature-time fire curves. This incorporates the compartment characteristics and also considers the cooling phase.

Pettersson et al. introduced temperature-time curves that relate the gas temperature within the compartment to its characteristics: the model considered the thermal properties of the compartment boundaries, the available ventilation and the fuel load [8]

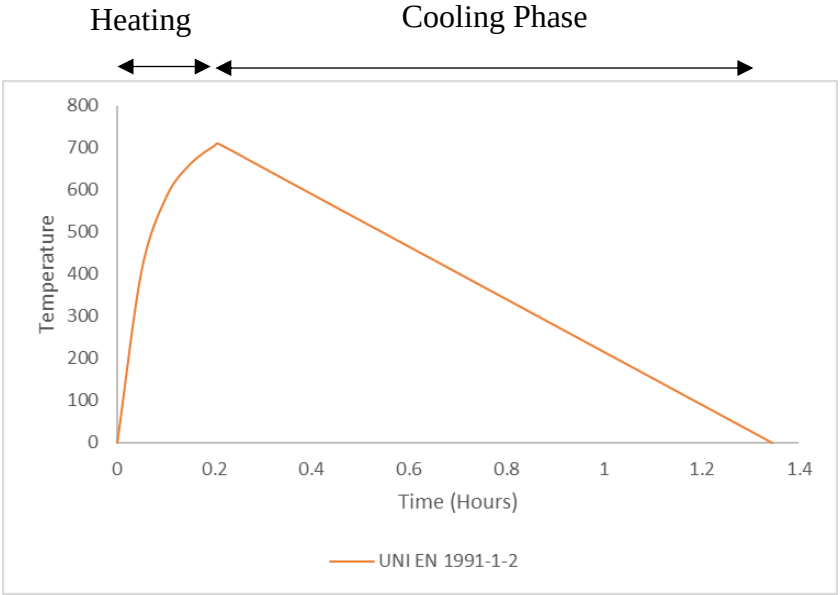

Fig. 8 A Typical Parametric Fire Curve

1.3.5. Basic Structural behavior under fire

Heat induced thermal expansion due to uniform temperature rise is given by

$$\varepsilon_T = \alpha \Delta T \tag{1}$$

Where α is coefficient of thermal expansion and ΔT is the temperature rise.

In a simply supported beam with length, there is no axial restraint. So, the new length will be $l\alpha\Delta T$ Fig. 9. This will be only thermal strain and no mechanical strains will generate. Hence, no stresses will develop in the element.

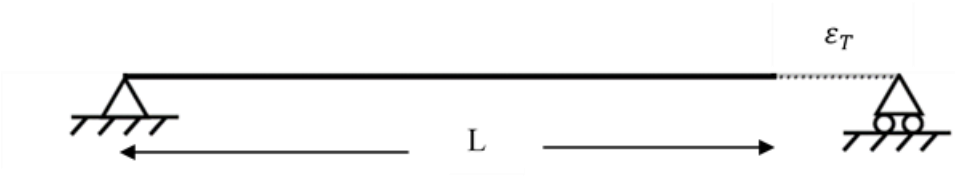

Fig. 9 Uniform heating of simply supported beam

If the beam is restrained, thermal strain will be zero ε_T. Since no displacement is allowed. This thermal expansion in the beam will be countered by an equal restraining force P, which will develop due to the end reaction. Thus, total strain ε_t will be the mechanical strain ε_m caused by this force.

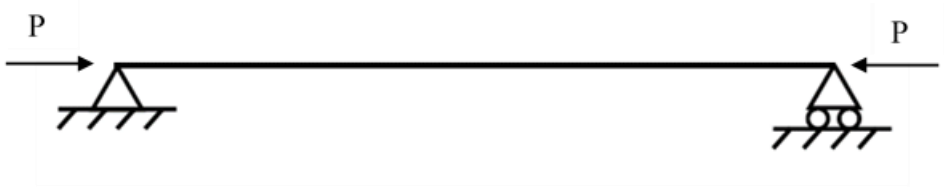

Fig. 10 Uniform heating of a restrained beam

$$\varepsilon_t = \varepsilon_T + \varepsilon_m$$

$$\varepsilon_t = 0$$

$$\varepsilon_m = -\varepsilon_T$$

The Axial load can be given by

$$P = EA\varepsilon_m = -EA\varepsilon_T = -EA\alpha\Delta T$$

If continued heating, the beam may buckle or yield, based upon slenderness of the section. It can also go under a complex response consisting of combination of both.

However, in real structures, floor beams are partially restrained by the columns. Therefore, the change in length will be less then given in Eq. 2. The restraint provided by the column can be replaced with a translational spring composed of the same stiffness as the column as seen in Fig. 11. The stiffness of this spring is called k_t.

In this case compressive axial stress will be given by

$$\sigma = \frac{EA\alpha\Delta T}{(1 + \frac{EA}{k_t L})} \tag{2}$$

And the critical buckling load will be

$$\Delta T_{cr} = \frac{\pi^2}{\alpha\lambda^2}\left(1 + \frac{EA}{k_t L}\right) \tag{3}$$

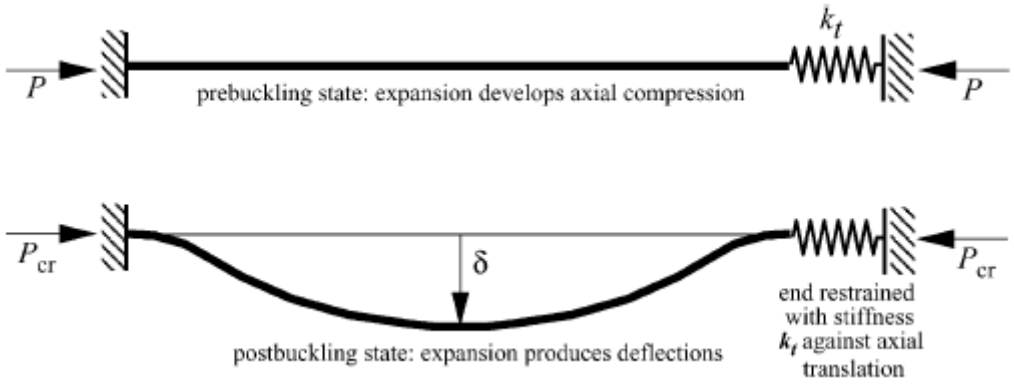

Fig. 11 Heating of beam with finite restraint [9]

In real fie scenarios, the temperature of the structure is not uniform. The rise in temperature depends upon the material and geometry of the element. For example, a concrete slab heating from the bottom, will have very high temperature on bottom. While the temperature on the other face will be very low. This will cause very high temperature gradient. The expansion on the lower surface will be much higher than the other side. This through depth thermal gradient causes thermal bowing that leads to curvature.

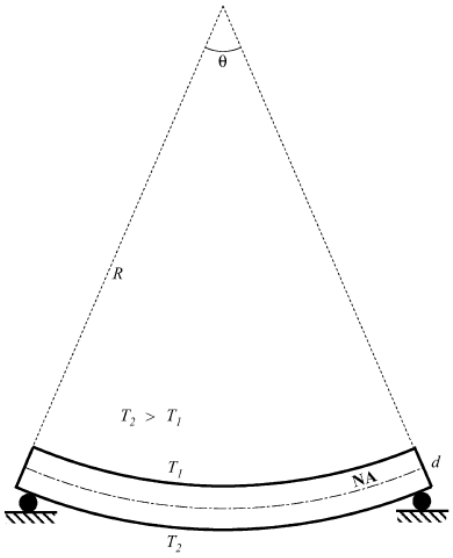

Fig. 12 Simply supported beam subjected to uniform thermal gradient [9]

This curvature as the result of thermal gradient (T_y) is given by

$$\phi = \alpha T_y$$

The strains developed due to curvature ε_ϕ can be given by

$$\varepsilon_\phi = 1 - \frac{Sin\left(\frac{l\phi}{2}\right)}{\frac{l\phi}{2}} \quad (4)$$

Thermal expansion and thermal bowing result in large deflections. Even at large deflections, a range of stress states may exist, depending upon the temperature distribution and material properties of the element. Deflection due to restrained expansion results in compression and deflection due to thermal bowing results in tension.

The effective strain due to combination of thermal expansion and thermal bowing is given by;

$$\varepsilon_{eff} = \varepsilon_T - \varepsilon_\phi$$

Positive values of ε_{eff} imply compression and negative values imply tension in the member.

1.3.6. Tall Building Failure Mechanism

1.3.6.1. Strong Floor and Weak Floor Mechanism

After the events of 9/11, there have been a lot of numerical research to understand the structural response of tall buildings subjected to multiple floor fires. Usmani et al. presented the strong floor and week floor mechanism [10]. The week floor mechanism starts from the fire floor, which goes under axial compression and flexure. The fire floor collapses under these loads and all the load is shifted to adjacent floors which fail and the failure progresses to all other floors. This failure can be controlled if a floor can withstand this loading. While in strong floor mechanism, floors are strong enough to withstand these loadings and prevent this progressive collapse. [10].

Lange et al. studied the collapse mechanism of a 12-story composite steel frame structure using an idealized exponential fire curve. An upper bound temperature was set to 800 ^oC. Floor beam axial stiffness was varied for two models. He also developed a simplified methodology to determine limit load capacity of a tall building. Without intensive finite element modelling, this provides a tool to determine if a particular collapse mechanism may occur or not, in a frame structure [11]

Fig. 13 sows the deformed shape after the collapse of two models [11]. Initially, when the fire starts, thermal expansions in the floor push the column outwards. Once the floor deflects due to the thermal expansion and thermal bowing, it pulls the column inwards. The inward pull of the column exerts axial compressive force in the floor above and below the fire floor. In week floor model, floors above and below the fire floor start to buckle. This transfers the forces to the next adjacent floors subsequently. The column losses its lateral support and failure progresses to all the floors [11]

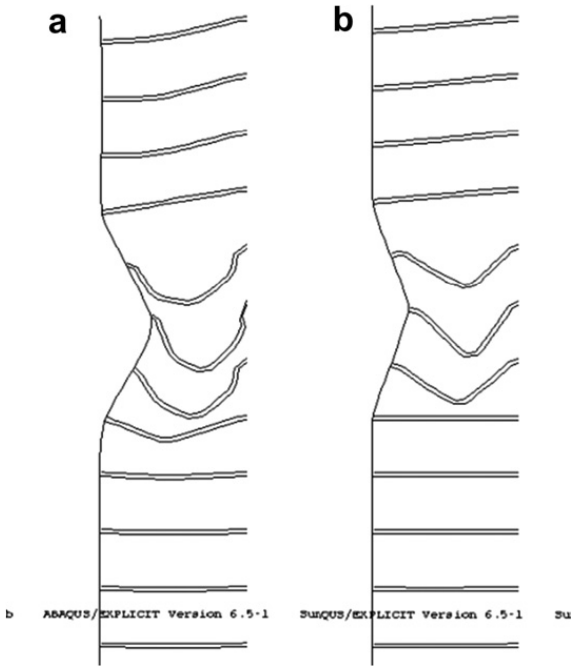

Fig. 13 Deformed shape showing two collapse mechanisms, a) Weak floor mechanism, b) Strong floor Mechanism [11]

In strong floor model, the column is initially pushed outwards due to the thermal expansion, but once it is pulled back, there is no progressive lose to the lateral support by adjacent floors. The column is pivoted to the adjacent floors and experience large moments. This continues until three hinges form as shown in Fig. 14. Once the plastic hinges form, column can no further support the floors and this may initiate the further collapse of the structure.

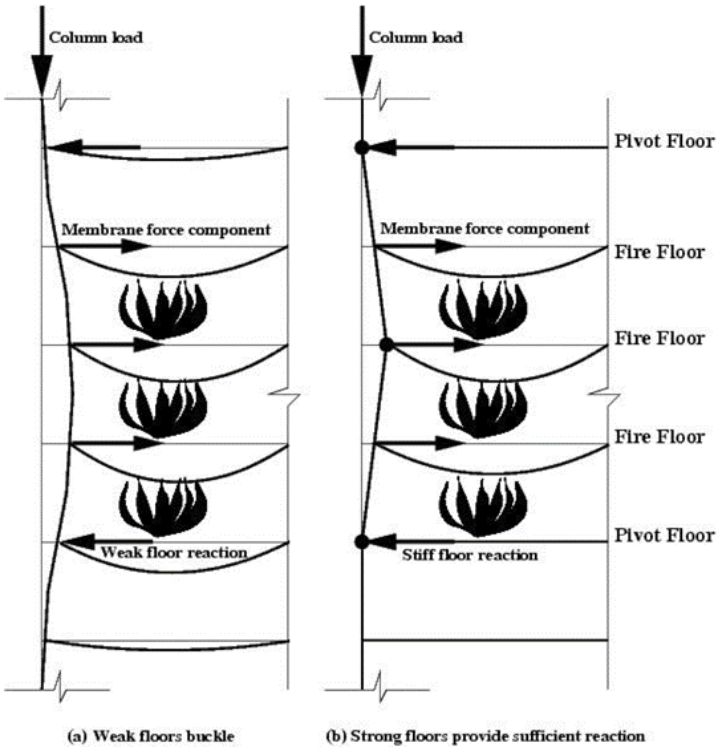

Fig. 14 Fire induced collapse of tall frames [11]

1.3.6.2. **Fire Resistance of Bi-linear Columns**

Bi-linear column are the columns which are not orthogonal to the floor plate. The use of bilinear columns is common in modern and innovative design of the buildings. Some of the existing and proposed buildings include: the WalkieTalkie, 52 Lime street and one Blackfriers.

The behavior of simply inclined columns is not different from the vertical columns [12] The performance of bi-linear columns was investigated by Law et al. [13]. They found out that bi-linear columns may lead to early failure of key structural elements even after following the design guidelines. They also presented a simple methodology to estimate the limiting temperature for the major elements of the structural system in order to deliver the required performance. The different arrangements of inclination and load transfer is shown in Fig. 15.

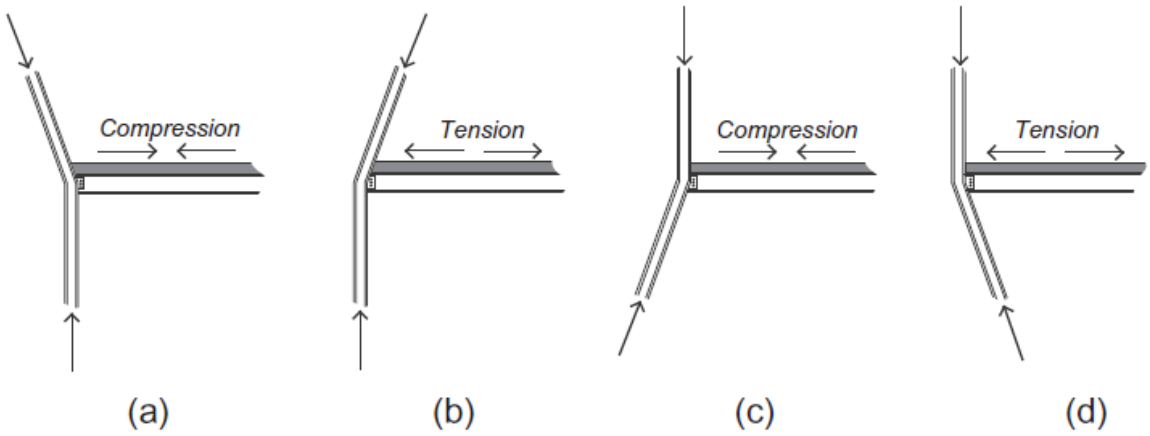

Fig. 15 Different structural arrangements for bi-linear columns [13]

The variables used in study were: the span of the slab between 10 m to 20 m, angle of inclination between -15 to +15, number of stories above the fire floor from 10 to 50 and section utilization from 75% to 95%.

When the floor plate was in compression, the failure occurred due to the formation of plastic hinge in the floor beam. When the floor plate was in tension, the failure occurred due to the plastic hinge formation in the column due to the expansion of the floor plate. The higher angle of inclination significantly reduced the fire performance of the structure. The number of floors above the fire floor also reduced the fire performance. Similarly, higher utilization also caused less fire resistance of the structure.

1.3.6.3. **Cardington Fire Test**

Several independent isolated experiments have been performed in different institutions over the years. Research involving full-scale experiments under natural fire, though, is minimal. One of the famous real-scale fire tests carried out on a realistic 8-story steel framed building that included six fire tests was the Cardington test. Such fire experiments were carried out between January 1995 and July 1996 at the Cardington laboratory in Bedfordshire, UK. The main goal of these fire tests was to determine the actions of structural elements under a natural

fire with real restraint. Data from the Cardington tests has been applied in several numerical studies and computational methods for verification and validation [14].

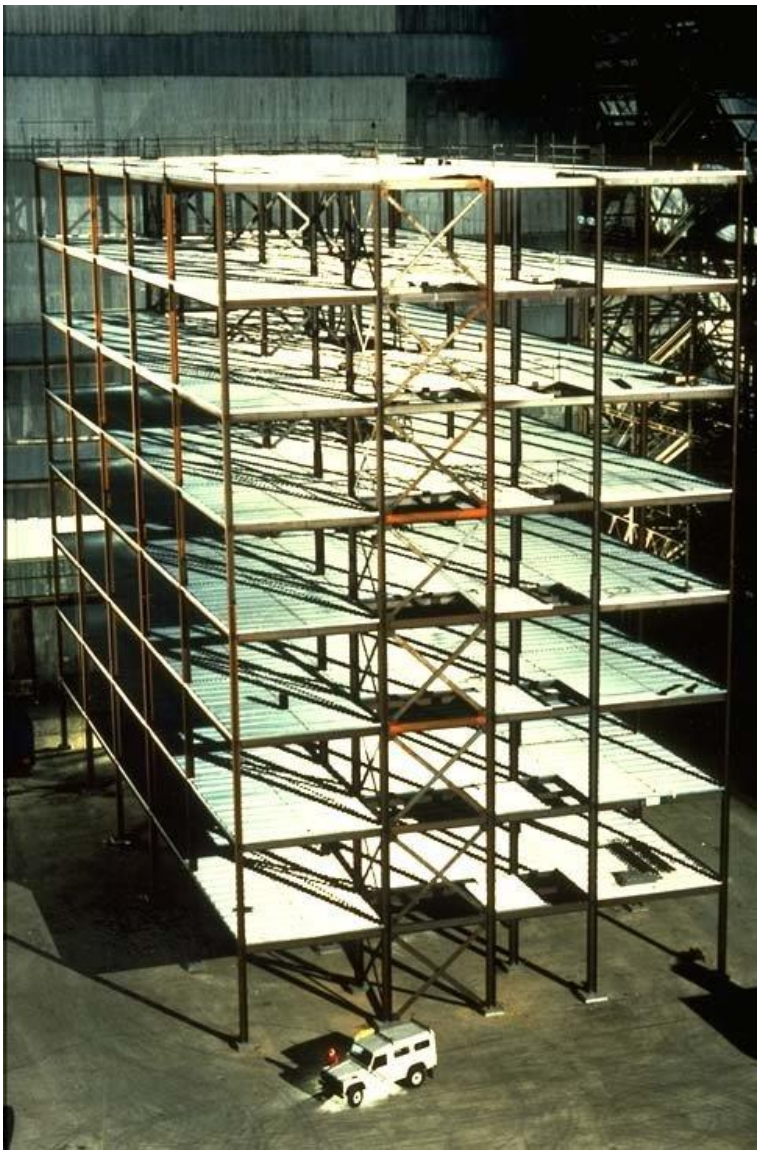

Fig. 16 Cardington test building prior to the concreting of the floors [15]

2. Methodology

A three-dimensional finite element model of a typical diagrid structure building was prepared to study its response under fire. The diagrid design followed for this study is based on work conducted by Jani et al. [3]. A range of fire scenarios were developed and results have been compared for different scenarios.

2.1. Building Description

The building has a layout plan of 36m x 36m and is 36 story high. The height of building is 129.6m with a center to center height of 3.6m for each floor. The diagrid angle is kept constant at 74.5^{o}. The spacing between diagrid nodes is 6m along the perimeter of the building. The design dead load is 3.75 kN/m^2 and live load is 2.5 kN/m^2. No other accidental load was applied to the building at the same time as fire.

The plan and elevation of the building is shown in Fig. 17.

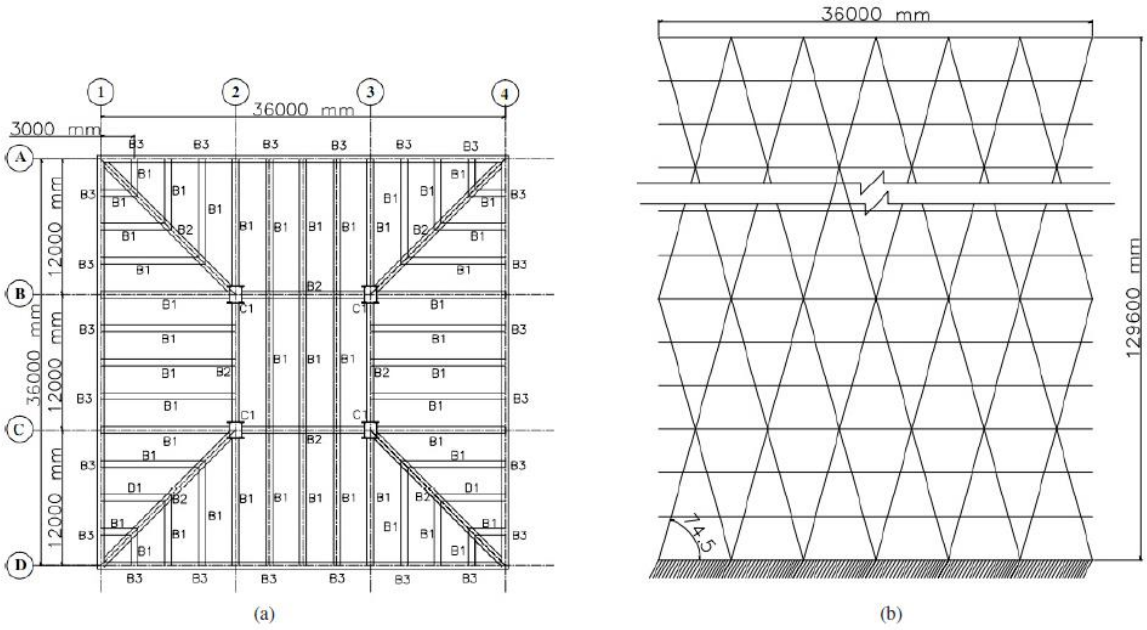

Fig. 17 Typical (a) Floor plan (b) Elevation [3]

2.2. Fire Modelling

The fire curve used for this study is ISO-834 fire curve. This fire curve is commonly used to test the fire response of individual elements, while whole structure behaves differently as proved by Cardington tests [16]. However, it can be used for the compartment fire to simulate a flashover. Although the assumption of uniform temperature in the compartment is not a realistic approach, and not necessarily the most critical one [17], it can give the preliminary idea of structural performance. Individual structural elements are subjected to the fire in 2D thermal analysis and then used in 3D modelling.

2.3. FEM Modelling

The full-scale testing of real structures is expensive and complex. Therefore, computational tools are often used to predict the structural behavior of complex structures under fire. The tool used for FEA simulation was SAFIR. The GiD preprocessor was used to create the input files.

2.3.1. Boundary Conditions

The diagrid system was clamped at the bottom by applying translational and rotational constraints in all directions. Diagrid nodes were assigned pin connections by applying the "Relaxation" condition to members joining at a node. This condition stops strong axis moment transfer across the connection. No changes were made to the beam-column joint, which attributes it to moment resisting properties. The continuity of slab was modelled by applying rotational and translational restraint, in horizontal direction, at the edge. Translation in the vertical direction was kept unrestrained.

2.3.2. Material Properties

SAFIR has a vast material library. It utilizes temperature dependent material properties which are in accordance to the BS EN 1993-1-2 for structural steel and BS EN 1992-1-2 for reinforcing carbon steel and concrete [18]. All the materials employed in this modelling have been employed from SAFIR material library.

The structural steel is STEELEC3EN. The modulus of elasticity for steel at an ambient temperature is 210 GPa. Poisson ratio is 0.3 and the yield stress is 250MPa.

The material for concrete used is SILCOETC2D [19]. A compressive strength of 30 MPa, Emissivity 0.7, Convection coefficient hot 35, Convection coefficient cold 4, and Poisson ratio 0.3 has been used.

Reinforcing carbon steel is STEELEC2EN in the material library of steel. Hot rolled class B steel reinforcement with #4 bars at 200 mm c/c spacing was considered in the slab. The reinforcement was provided in four layers; two on the bottom and two at the top, perpendicular to each other with 20 mm concrete cover. The modulus of elasticity of this steel at ambient temperature is 210 GPa. Poisson ratio of 0.3 and yield stress of steel has been considered 500MPa.

2.3.3. 2D Thermal Modelling

Thermal analysis was performed for all the structural members and run for two hours whilst being subjected to the standard fire curve. The output of thermal analysis of beam elements is saved as a temperature file called, ".TEM". This file contains the temperature history for each time step. Similarly, the temperature history of shell element/ slab is saved as .TSH file. These .TEM and .TSH files of all structural members are later assigned to the elements in 3D structural analysis.

a) Diagrid

The diagrid section used in the structure [3] changes from the bottom to the top. A circular pipe section of 450mm diameter with wall thickness of 25mm for lower 16 floors and 375mm with

wall thickness of 12mm for top 16 floors was used.

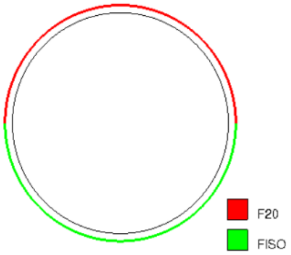

Fig. 18 Temperature constraint, diagrid section

The diagrid section was subjected to fire on half of the circumference and ambient temperature of 20 ^{o}C on the other face. The fire side will face inside of the compartment in 3D structural model. Void constraint was applied to the inner face of the section. Torsional analysis was also run in 2D thermal analysis to use this section in 3D structural modelling. The boundary condition for temperature applied in SAFIR is shown in Fig. 18. The temperature development in the inner and outer face of the diagrid is shown in Fig. 19.

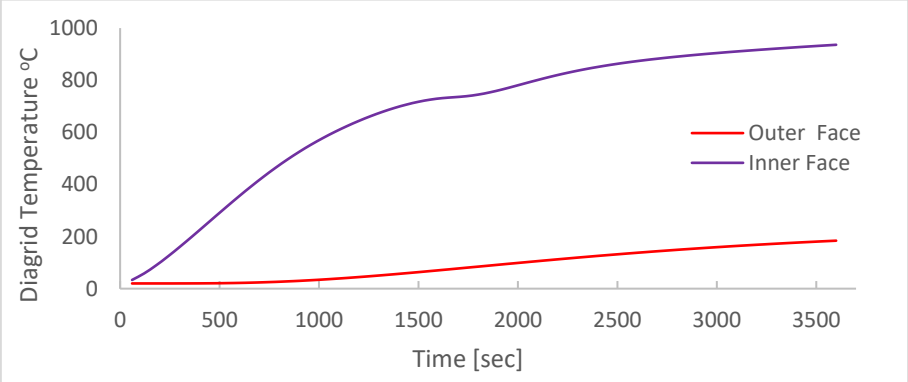

Fig. 19 Temperature development in the diagrid section

b) Column

The column section was simplified from the actual design for the ease of analysis. Square steel section of 1.5m x 1.5m with wall thickness of 50mm has been used for the column section. The column was subjected to fire on all sides. The void constraint was applied to the inner face of the hollow section and torsional analysis was run to use the section in 3D analysis. The internal columns can be seen on Grid B2, B3, C2 and C3 in Fig. 17

c) Beam

Two types of beam sections were used for the model: B1 and B3 = ISMB 550, B2 = ISWB 600. The layout of beams can be seen in Fig. 17.

The beam section was subjected to fire on all the faces except the top face which connects with slab. Composite action of beam and slab was achieved by assigning a slab section on top of beam in thermal analysis. Torsional analysis was also run in this model.

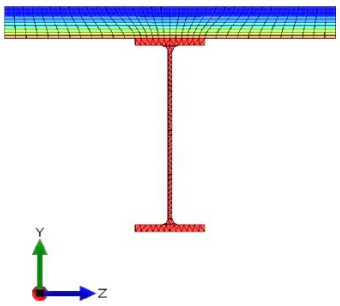

Fig. 20 Composite beam-slab section

Thermal analysis of the slab section was also run separately. This slab section over the beam was given the property of insulation material in 3D structural analysis, so that it doesn't affect the 3D structural analysis. The composite beam-slab section can be seen in Fig. 20. The temperature development in the web of beam ISWB 600 is shown in Fig. 21.

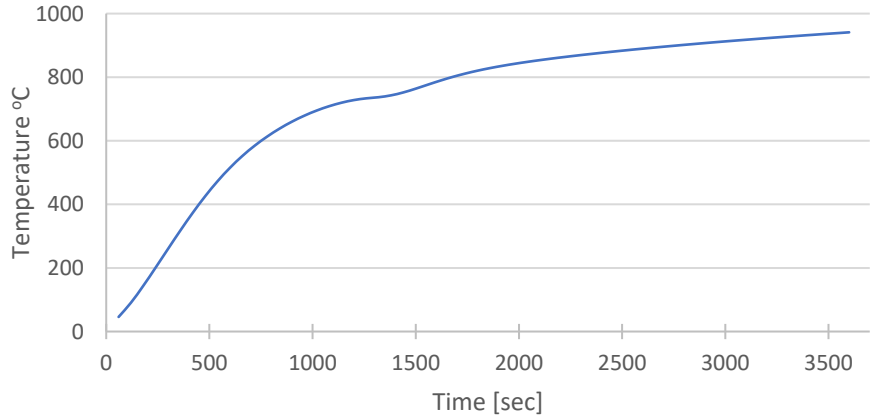

Fig. 21 Temperature development in the web of beam ISWB 600

d) Slab

RCC slab of 100mm thickness was used for the structure. Slab section was modelled by 4-node shell elements and section was divided in 8 surfaces over the depth. These surfaces are later used to get the output of stresses and strains in the slab. The standard fire curve was applied on the bottom face and an ambient temperature of 20 ºC was applied on the upper face of slab. Fig. 22 shows the temperature development in the slab section.

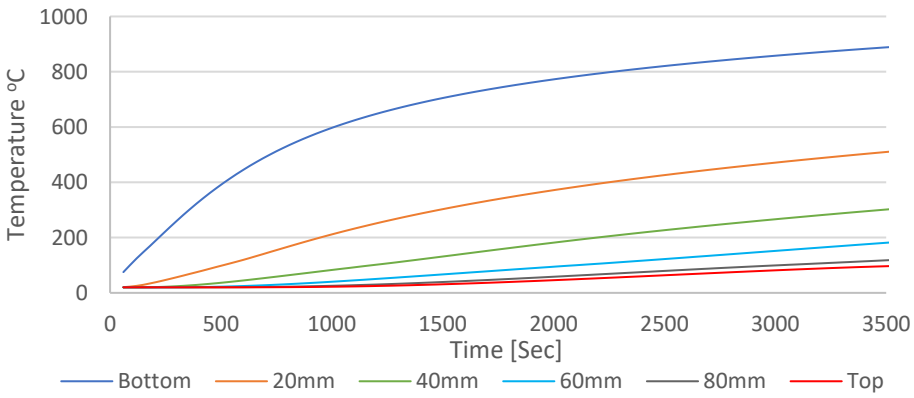

Fig. 22 Slab Temperature Development

2.3.4. 3D Structural Modelling

The 3D modelling was done using beam and shell elements. The temperature history of the structure is read from the files created during the temperature analysis. Three node quadratic beam elements with two points of integration were used to model diagrid and structural beams. Beam elements can predict the global behavior of structure and utilize less modelling and computational effort. Four node shell elements with four points of integration were used for the slab [18].

SAFIR needs a 4th node to describe the orientation of a cross section on a beam in the 3D model. While this was achieved in GiD by introducing the system of local axis to assign the section in the global 3D model. System of local axis was introduced to ensure the stronger axis in position and the location of fire facing side towards the inside of the compartment.

Two types of FEM models were created. Both the models are for 6 floors in height whilst having different floor areas. The load of upper floors was applied as nodal load to the top of columns. The load was applied under the command FLOAD, which gradually applies the load in 20 seconds. Dynamic structural analysis was run separately to calculate the load of upper floors.

Dynamic analysis was run for all the models because local failure of a structural member that does not affect the safety of the whole system can be handled by this. In SAFIR, automatic adaptation of time step is possible in dynamic analysis and structural calculation continues until failure occurs or when the maximum deflection reaches a defined value input by the user [18]. The analysis was run considering TIMESTEPMIN of 2.0E-5 sec for convergence.

No exclusive modelling was done for the connections. Hence no failure occurs at the connections. As the purpose of the study is to see the response of a diagrid structure, this method is considered to be a reasonable approach. Only the upper slab in the fire compartment has been considered for heat transfer. It has been assumed that floor finish on lower slab in fire compartment provides enough insulation to the lower slab in fire compartment. Also, only the diagrid section in fire floor has been subjected to the fire and no heat transfer has been considered from this section to the upper and lower floor diagrid via connection. Moreover, all the structural members have been assumed to be unprotected.

a) Strip Model

The strip model is the modelling of one third of the floor area. Floor 1-6 have been modelled and a load of 30 upper floors has been applied as nodal loads. Two fire scenarios have been created one for mega floor F3 and one for intermediate floor F4. The modelled area is shown in Fig. 23. Mega floor F3 is highlighted by dark line in the figure on the right. The boundary conditions have been explained in Section 2.3.1. Initially, the translation and rotation were restrained at the grid line 2 and 3 but this does not reflect the dynamics of structure ideally. It was planned to run the model again by changing this condition to unrestrained and see the output but this could not be completed. However, the primary focus in strip model is the response of diagrid structure at grid A and D, which is not expected to be affected by this condition. The total floor span in longer direction is 36 m and 12 m in shorter direction.

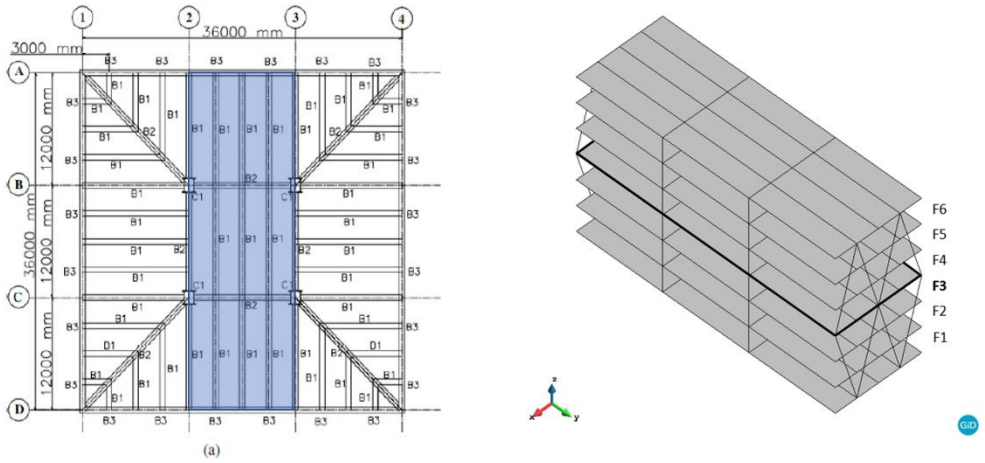

Fig. 23 Strip Model

b) Corner Model

The corner model is the modelling of one quarter of the floor area of the floor plan and includes floor 31-36. Floor F33 is the mega floor. Two fire scenarios with standard fire have been created one for the mega floor F33 and one for intermediate floor F34. The model can be seen in Fig. 24. The total floor span in both directions is 18m.

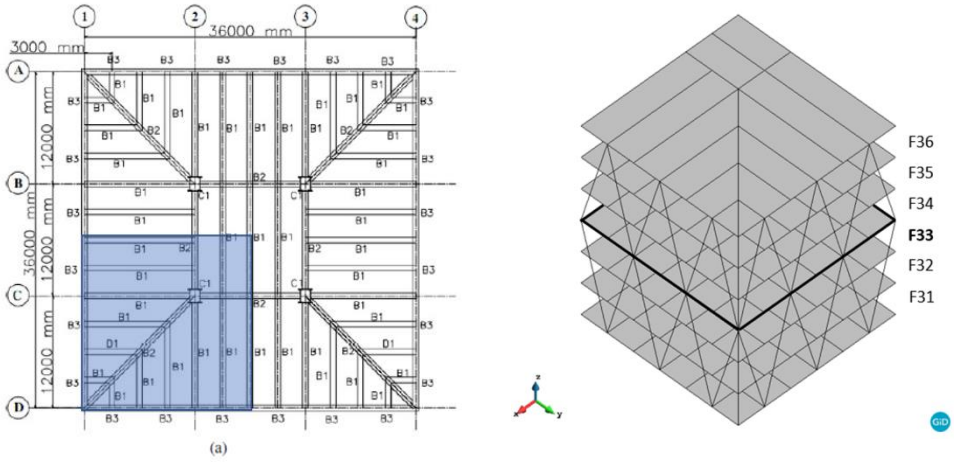

Fig. 24 Corner Model

2.3.5. Fire Scenarios

It was proposed to run multiple fire scenarios. This included at least 4 fire scenarios for each model under ISO-834 fire and four under parametric fire to see the effect of cooling phase also. This would have resulted in total of 16 fire scenarios. Unfortunately, due to work stoppage only four fire scenarios could be completed.

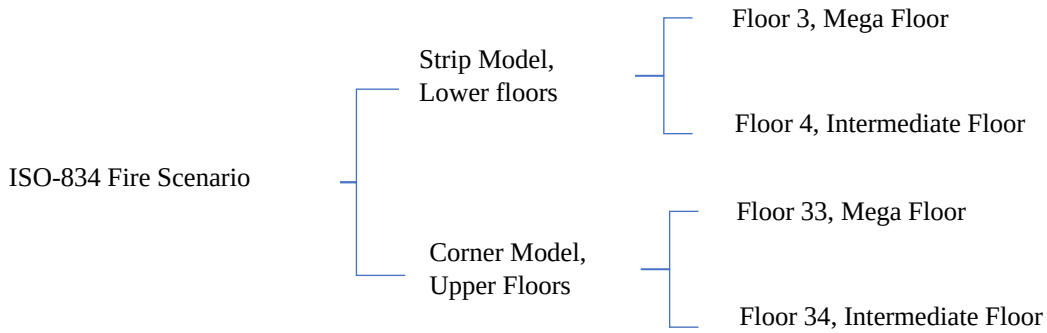

2.3.6. Mesh Sensitivity

Various models were run by refining the mesh. Considering variation of results and simulation time an optimal mesh size was finalized. The corresponding beam element size is 0.3m and shell element of 1m×1m.

3. Results

3.1. Overall Response of the Structure

As the fire starts, thermal expansion takes place in the floor plate and the diagrid is pushed outwards. Continued heating generates thermal gradient in the floor which creates thermal bowing. This slab deflection generates extra P-δ moment in the slab due to the restraint provided by the diagrid on the ends. As the time passes, gradual increase in the thermal load

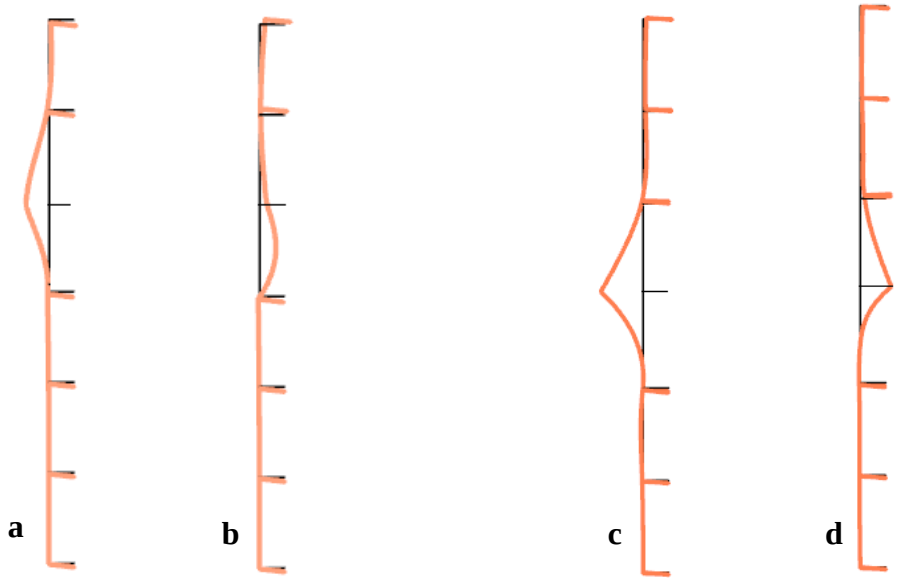

Fig. 25 Push out and pull in of diagrid (×30), intermediate floor fire (left), mega floor fire (right)

and extra P-δ moment increases the slab deflection. Larger deflection in the slab reduces the push force and thus effect of thermal expansion diminishes. Excessive deflection results in pull back of the diagrid. The diagrid crosses its initial position and bends inwards. The deformed shape of diagrid as the result of this push out and pull in phenomena is shown in Fig. 25. Strip model for intermediate floor fire scenario is on the left (a, b) and strip model mega floor fire scenario deformed shape is on the right (c, d).

As the fire floor is pushed outwards, axial compressive forces develop in the fire floor due to the restraint provided by the diagrid and axial tensile forces develop in the floors above and below the fire floor. These forces are maximum in the floors adjacent to the fire floor and reduce as we move to the farther floors.

3.2. Intermediate Floor Fire

The lateral displacement of diagrid; axial force in diagrid and mid-span floor beams is shown in Fig. 27.

It can be seen in Fig. 27 (a) that initially the diagrid is pushed outwards and the maximum displacement reached is 31 mm at 700 sec. At this time there are maximum compressive forces in the floor and past this point the axial forces in the floor start to reduce.

Fig. 27 (c) shows the upward displacement of the diagrid. Initially, the diagrid is shortened 4-6 mm because of the mechanical load of the structure. Around 700 sec, due to the thermal

elongation, it moves upwards passing its initial position to about 1 cm higher. Fig. 27 (b) shows, due to the thermal strains, axial load in the diagrid increases in time from 700 to 1724 sec.

As the thermal gradient increases in the floor, it deflects downwards. The floor experiences high compressive forces, Fig. 27 (d), due to the end restraint and flexural stresses due to the bending. The continued deflection diminished the push force of thermal expansion and pulls the diagrid inwards. The diagrid's inward displacement is relatively low when compared to the outwards displacement. This displacement of the diagrid depends on the relative stiffness of the diagrid and floor beam sections. The diagrid experiences high axial and bending forces and at 3580 sec the diagrid buckles at the lower level.

Fig. 26 shows the development of moment along the height of the diagrid in four time intervals. At 60 sec, as the thermal expansion takes place in the floor, it starts exerting force on the diagrid. A positive moment is generated in the diagrid at floor 4 and negative moment at the level of floor 5 which creates tension in the floor 5. These moments are maximum at 700 sec when the axial forces are also maximum in the floors. At 1724 sec, the moment reduces and starts reversing its direction. At the time 3580 sec, just before the buckling of diagrid, there is negative moment on the floor 4 and positive moment at floor 5. This is due to the shift of force interaction between diagrid and floor. The positive moment at floor 4 shows the tensile forces in the floor and pull in of the diagrid. The floor 5 provides the lateral restraint to the diagrid, thus it goes in compression and creates positive moment.

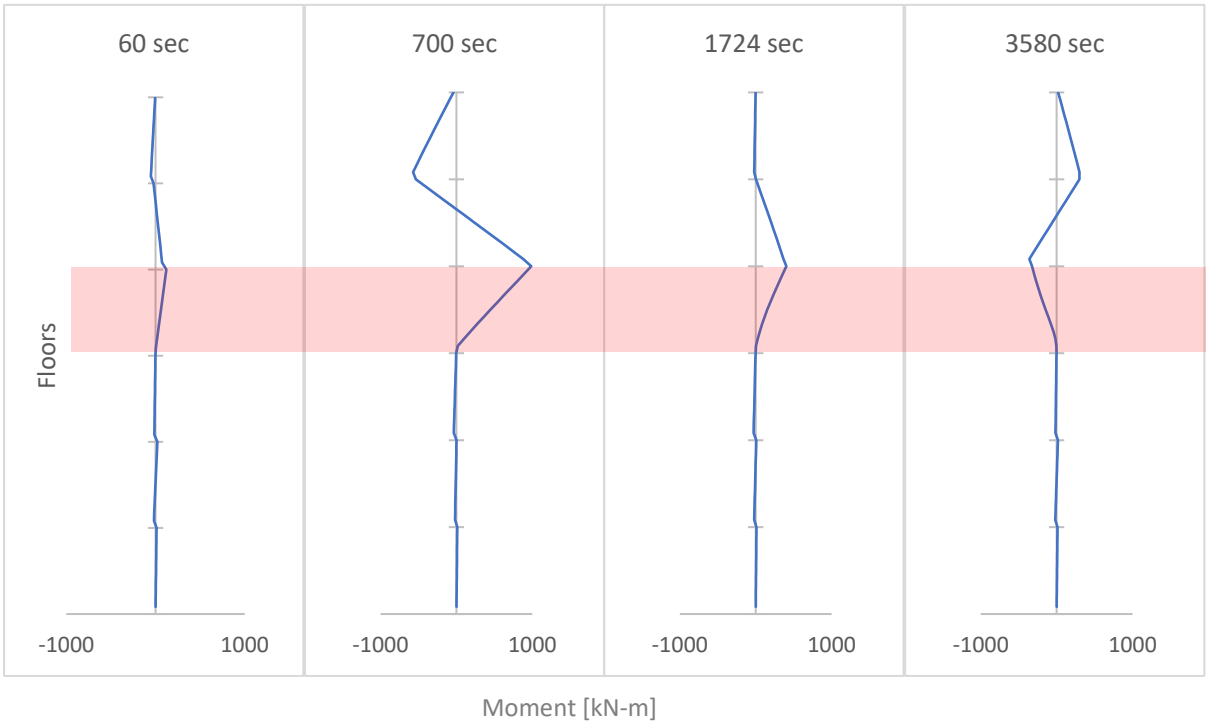

Fig. 26 Moment along the height of diagrid, Strip model, Floor 4 (F)

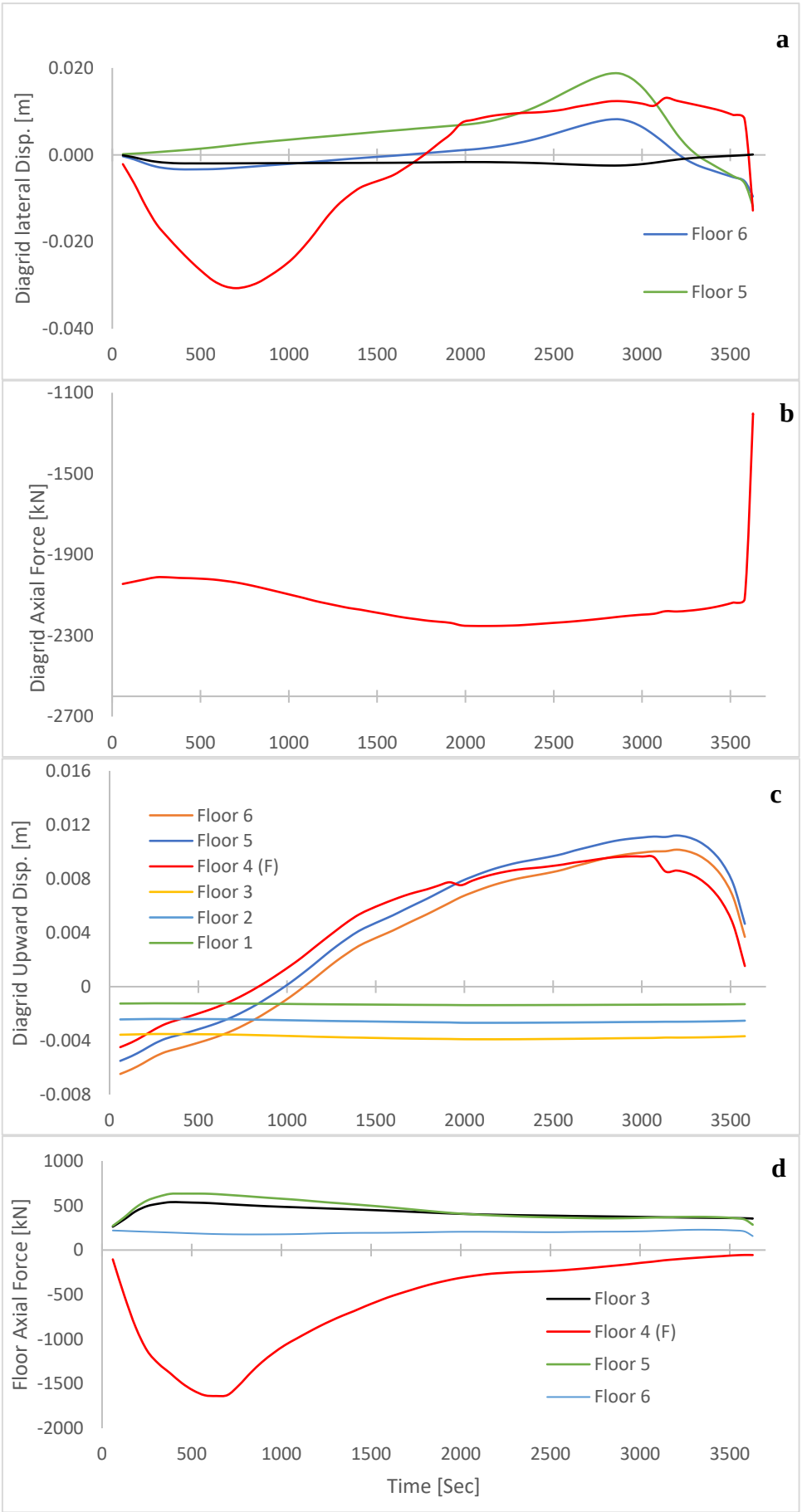

Fig. 27 Displacement and forces in Intermediate floor fire, Strip model

The connection at the floor 3 is a pin connection, so moment is not transferred to the lower floors. This reversal of axial forces in not very prominent in Fig. 27 (d) for axial forces in the floor. The axial forces in Fig. 27 (d) have been plotted for the mid span beam element at all floors while it changes throughout the length of the beams because of the interaction with internal columns. The flexural stiffness of the columns is much higher than the diagrid section, which provides higher restraint to thermal expansion of beams.

- Flexural Stiffness (EI) of Column 2.14E+10 Pa-m^4
- Flexural Stiffness (EI) of Diagrid 1.59E+08 Pa-m^4

Moreover, the beam column connection is moment resistant, which resists beam rotation at the face of column. Fig. 28 shows the structural layout of beams followed for the analysis. Fig. 29 shows the plot of axial forces in the fire floor at two time steps; 700 sec where the displacement and axial forces are maximum in the structure and 3580 sec which is the time step before failure occurs.

Fig. 29 shows that maximum axial compressive forces are developed in Beam 1. Initially at 700 sec, Beam 1 experiences lower compressive forces in Bay 1 and 3 while maximum compression forces in Bay 2. This is due to the high flexural stiffness of the column which restrains the thermal expansion of the floor beams. After the pull in of the diagrid, tensile force is experienced in Beam 1 in Bay 1 & 3 while it remains compressive in Bay 2. Lower axial compressive forces are experienced in the Beam 2 & 3 at 700 sec, while at 3580 sec, Beam 2 experiences tensile force at the mid span of all bays and Beam 1 has tensile forces in the midspan of Bay 1 and 3 only.

This effect of column's stiffness is also prominent in the deflection of slab. The beams in Bay 1 & 3 are restrained against rotation on one side while the beams in Bay 2 face the restraint on both sides. Fig. 30 Deflected shape of slab (x5) shows the deflection of slab. Deflection is maximum in Bay 1 & 2. The maximum deflection in the mid span of Bay 2 is 902 mm and is 988 mm in Bay 1 & 3.

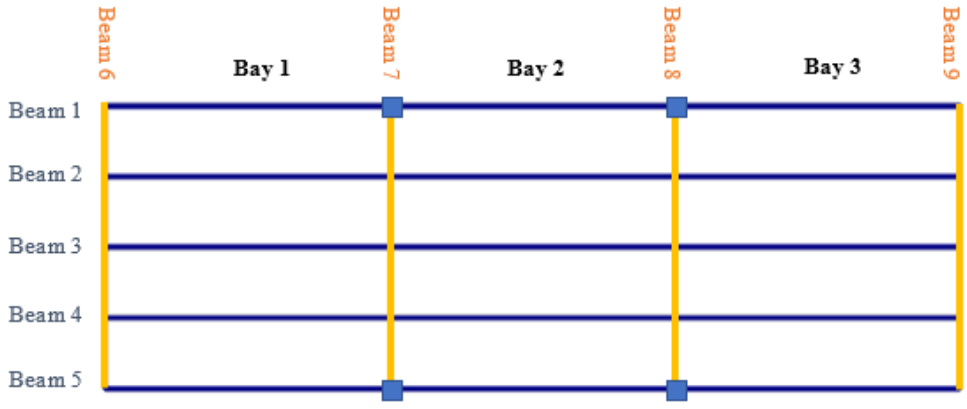

Fig. 28 Structural layout for Analysis

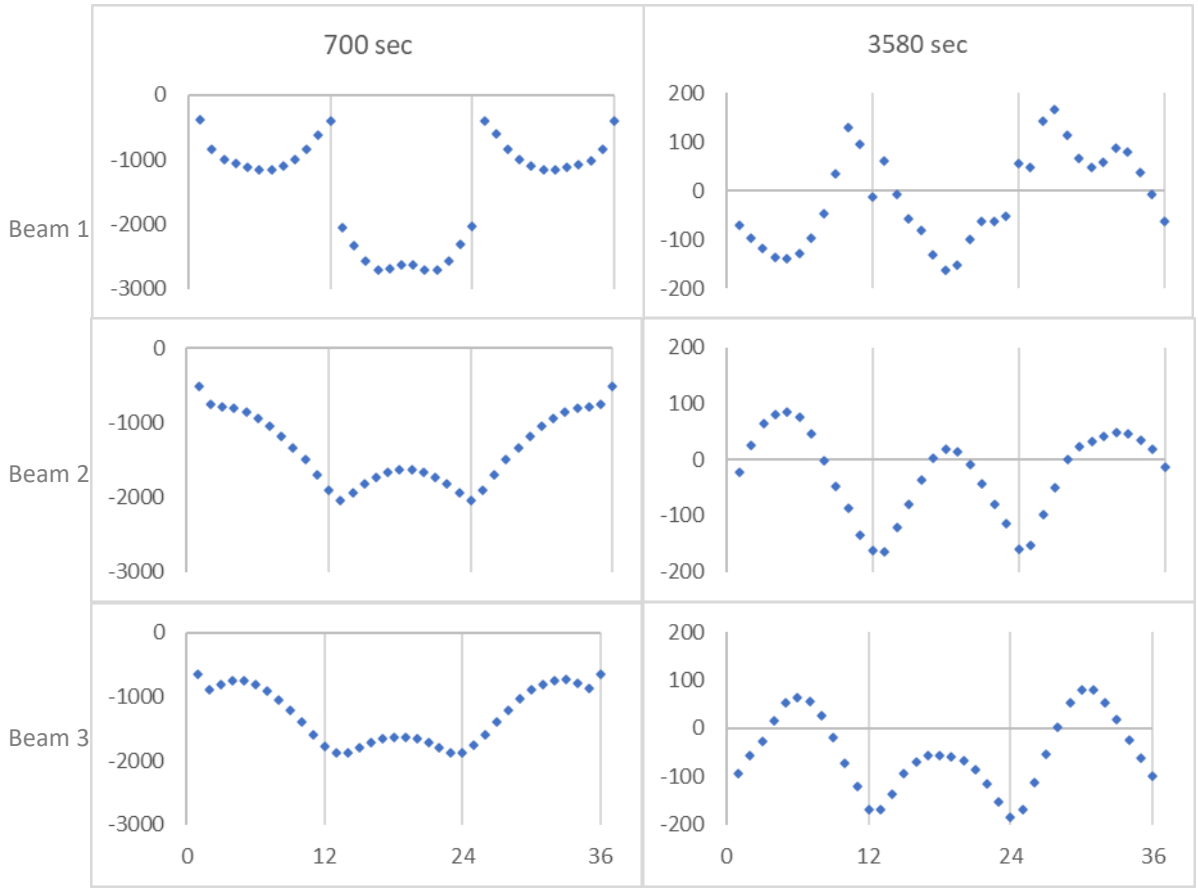

Fig. 29 Axial forces along the beam length at start and before failure. Strip Model Y-axis=Axial Force (kN) X-axis = Beam length (m)

The Beams in the Bay 2 remain mostly in compression under thermal expansions. Therefore, only thermal strains develop in Bay 2. While in Bay 1 and Bay 3 tensile strains also generate besides thermal strains. Due to the combined effect of thermal and tensile strains, the deflection is larger in Bay 1 & 3. It can be interpreted from this data that catenary mechanism develops in Bay 1 and Bay 3 as explained by Lange et al. [11]. However, in the Bay 2 the deflection is caused by thermal expansion and thermal bowing and no catenary forces develop.

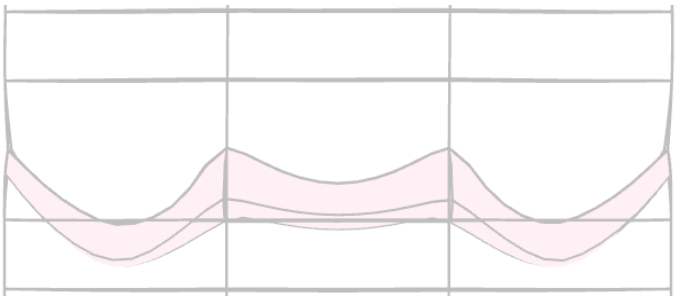

Fig. 30 Deflected shape of slab (x5)

Fig. 31 shows the bending moment developed in the mid-span of each bay of fire floor. It can be seen that maximum positive moment is developed in Bay 2. This is due to the higher restraint provided by the columns to the thermal expansion of the floor beams.

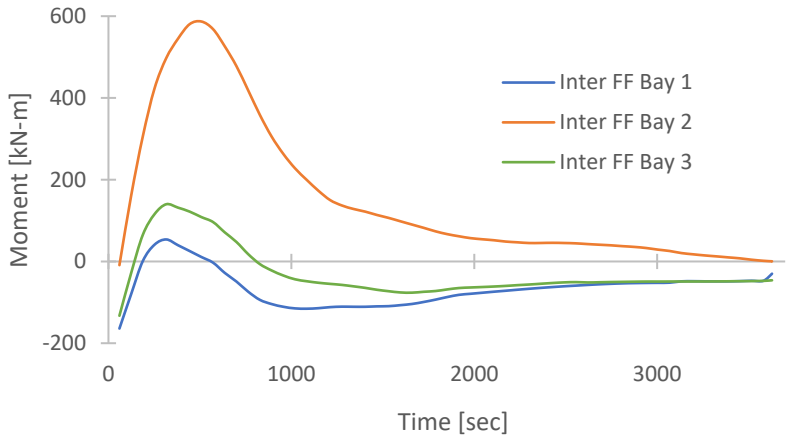

Fig. 31 Bending moment in each bay of fire floor

In the case of the corner model intermediate fire, the floor 34 is on fire and does not have very high loads from the upper floors. Therefore, very low axial forces in the column. Fig. 32 shows the axial force in the diagrid on fire Floor 4 and 34.

The size of the diagrid section reduces from 450 mm to 375 mm in external diameter. Overall, the fire response of the structure is similar to the strip model but it fails due to the large thermal deflections in the slab.

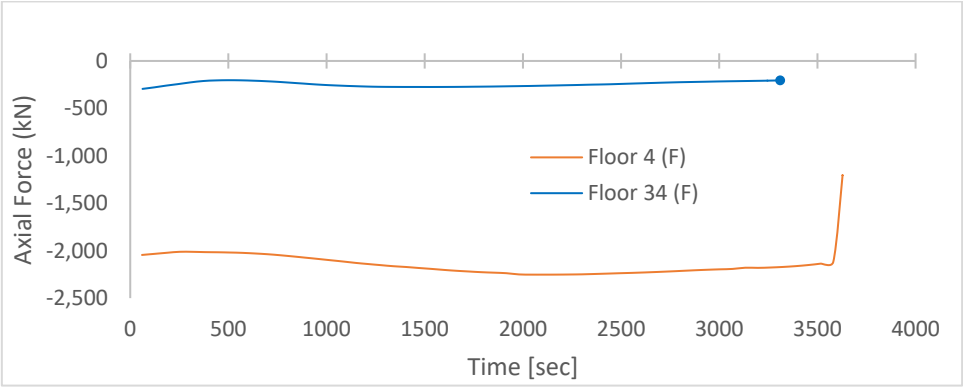

Fig. 32 Axial force in the diagrid

Fig. 33 shows the lateral displacement of the diagrid in the corner model. Data shows that the lateral displacement occurs in the fire floor only while in the other floors this is negligible as compared to the strip model. This is because of the lower stiffness of the diagrid section. The axial forces are also very low due to no significant load from the upper floors. But due to the less stiffness of the diagrid it is pulled inside more as compared to the floor 4 fire. As the result of lower stiffness, the floors adjacent to the fire floor experience lower axial tensile force.

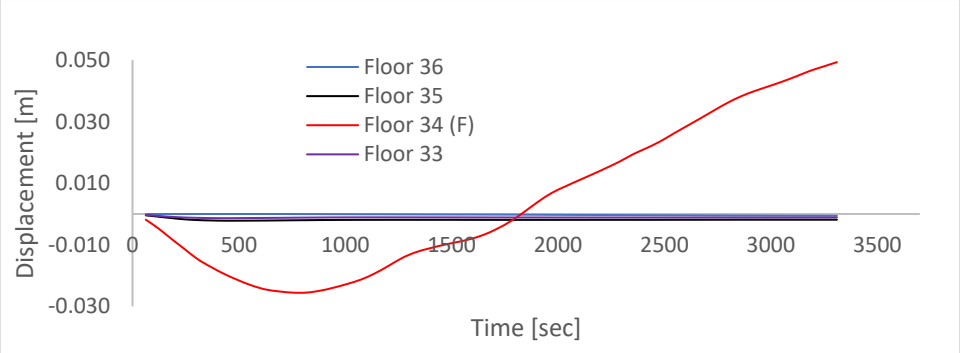

Fig. 33 Diagrid lateral displacement, Corner model

Fig. 34 shows the axial force development in the mid-span of the fire floor and the floor above the fire floor. The plot shows that the axial forces in the case of corner model, are almost the same to strip model in the fire floor. While axial forces when compared for the above floor, they are 40% higher in strip model than the corner model.

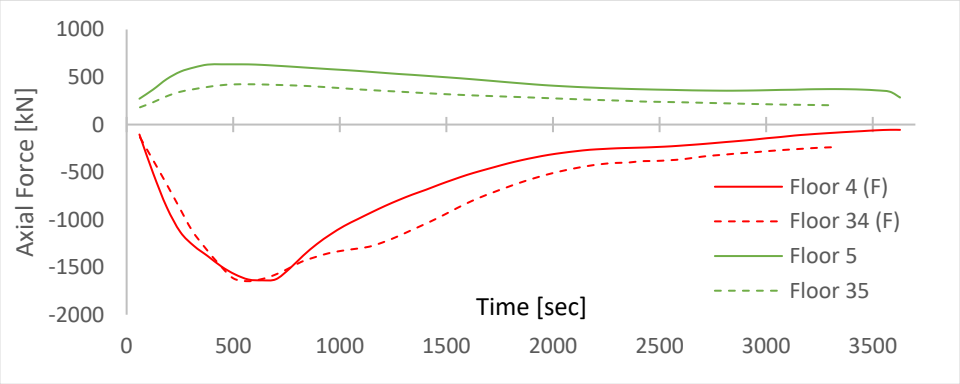

Fig. 34 Axial forces in fire floor and the floor above, Corner model

3.3. Mega Floor Fire

The overall structural response in case of mega floor fire is similar to the intermediate floor fire. Initially the diagrid is pushed outwards which generates axial compressive forces in the fire floor and axial tensile forces in the floor above and below the fire floor. However, it takes longer to pull back the diagrid to its initial position, and once it reaches the initial position, it quickly bends inwards.

Fig. 37 shows the diagrid displacement and axial forces in the structure. Fig. 37 (a) shows that the diagrid maximum lateral deflection is 42 mm and it occurs at 830 sec. At this time there is a maximum axial force in the diagrid of 1,972 kN Fig. 37 (b). Fig. 37 (d) indicates that the axial force in the fire floors reaches its peak a bit earlier, that is because it has been plotted only for a mid-span beam element, while it changes from beam to beam due the interaction with internal columns as shown in Fig. 29. However, the trend is almost the same. Beyond this point, as the slab starts to deflect, the diagrid is pulled back and axial forces start to reduce.

An interesting trend is observed at 2430 sec, where there is a sudden change in the forces and displacement. The diagrid is pulled inwards by 44 mm in 90 sec. The axial force in the diagrid drops from 1,820 kN to 1,755 kN and vertical displacement of the diagrid falls from 11 mm to 8 mm.

Though this pattern seems like a plastic hinge has formed in the diagrid at the floor above and below but the values of displacement and forces in the diagrid do not change significantly. Moreover, the moment in the diagrid at this point is much lower than the plastic moment capacity of the section. The diagrid section is heated from the inside of compartment. Fig. 19 shows the temperature development in the diagrid inner and outer face. Therefore, it is difficult to determine the exact plastic moment capacity of the section. However, for the conservative approach, the plastic moment capacity has been estimated for the inner face temperature. Plastic moment for the diagrid section at 850 ^{o}C is 769 kN-m. While the moment in the diagrid at Floor 4 is 173 kN-m and in Floor 2 is 158 kN-m. Fig. 29 shows the development of bending moment and axial force in the diagrid at floor 2 and 4.

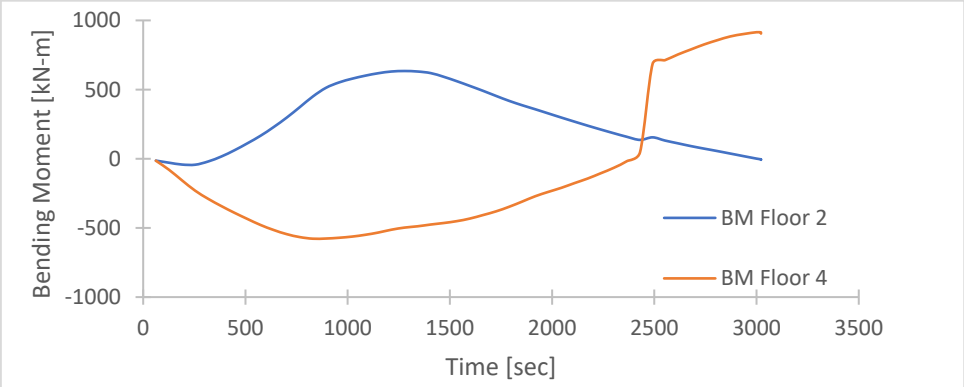

Fig. 35 Bending Moment and Axial force in Diagrid section at above and below the fire floor

To investigate the reason of this behavior, bending moment was plotted in Beams 1-3 in Bay 1 at mid-span and on the edge towards the diagrid Fig. 36.

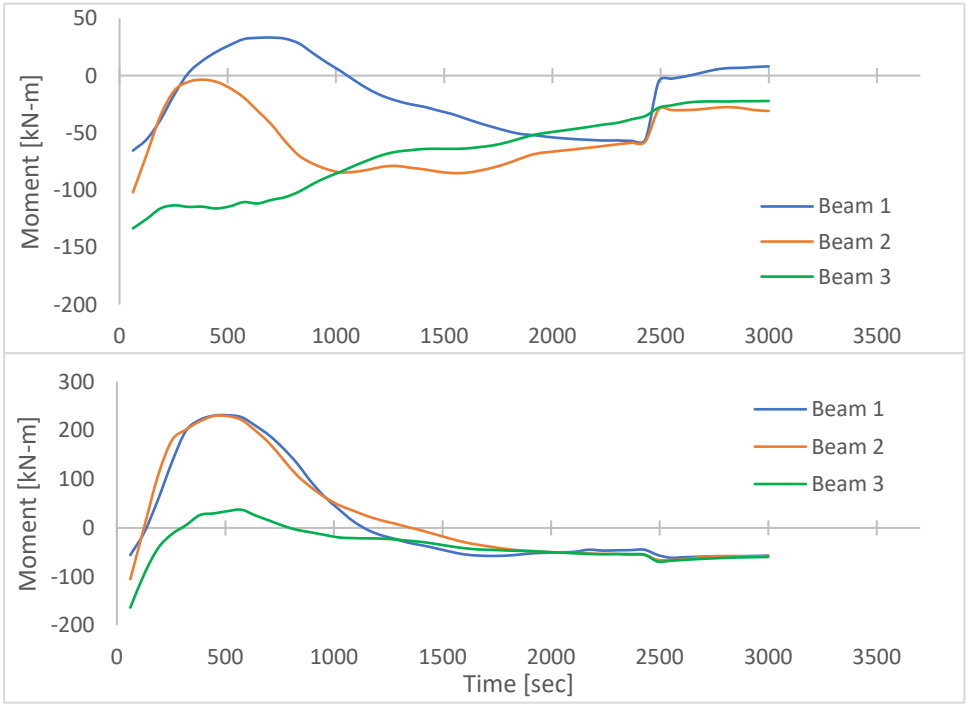

Fig. 36 Bending moment in Bay 1 of fire floor, edge elements (above) mid-span elements (below)

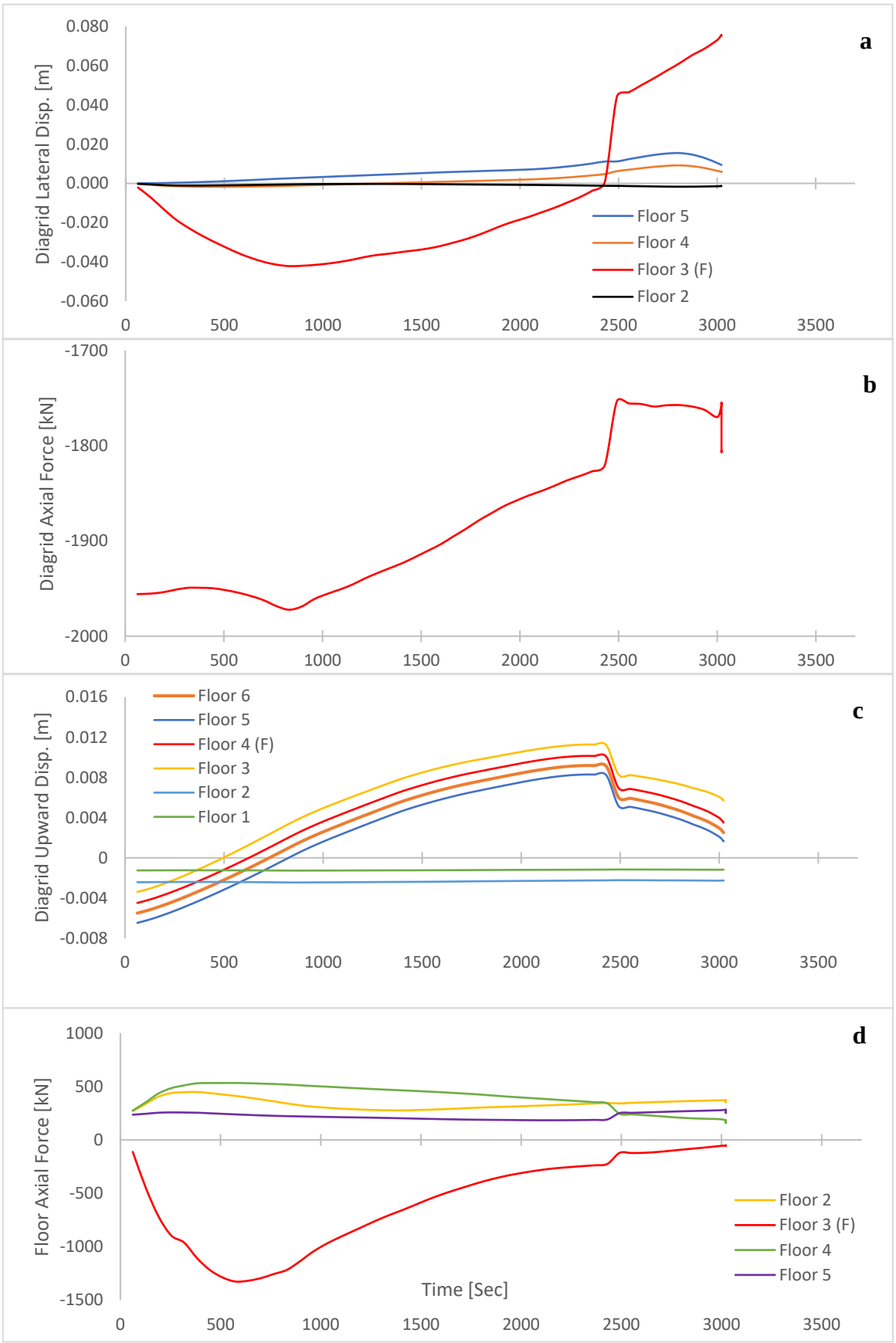

Fig. 37 Displacement and forces. Strip model, Mega floor fire

Fig. 36 shows a sudden drop in bending moment to zero in Beam 1 of edge element. The moment in Beam 2 and 3 reduces but does not approach to zero. While the moment at mid-span of these beams increases slightly. The temperature in the web of beam is approximately 878 ^{o}C and thus plastic moment capacity is 52 kN-m. The moment in Beam 1 drops from 54 to zero. This indicates the formation of plastic hinge in the beam elements close to the edge (i.e. Beam 1 & 5). This results in sudden increase in slab deflection and higher pull in force in the diagrid and subsequent inward displacement of the diagrid. However, beyond this point, stresses are redistributed in the floor and it stabilizes.

This pattern was not seen in the corner model mega floor fire. This pattern could be understood better if there were more simulations run for the strip model mega floor and multiple floor fire.

However, past this point at time 2491 sec, it starts taking load again. The increase in temperature results in reduction of flexural capacity of the floor. At time 3021 sec the floor fails due to high thermal deflection. The maximum deflection in Bay 1 reaches 1.2m and the diagrid is pulled inside up to 75 mm.

Fig. 38 shows the lateral displacement of the diagrid section in corner model. Part b shows the similar trend to the corner model in the intermediate floor fire. There is no significant displacement int the floor above or below the fire floor because of the lower stiffness of the diagrid section.

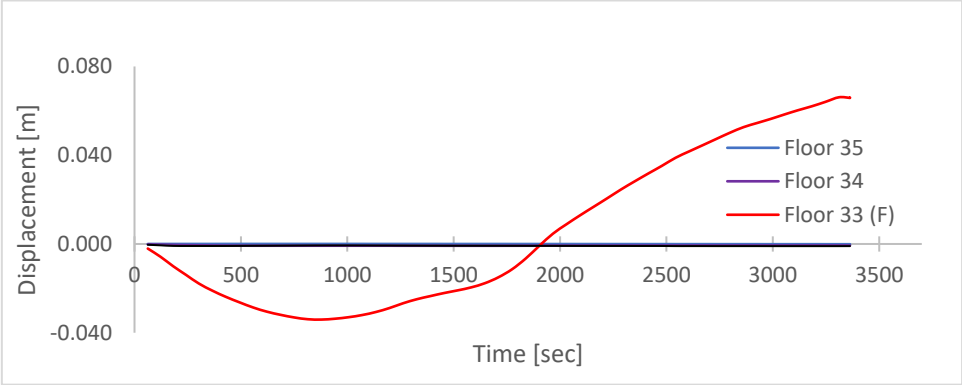

Fig. 38 Diagrid lateral displacement, Corner model

3.4. Comparison of Models

Fig. 39 shows the lateral displacement of the diagrid for all the scenarios. The data shows a significant difference where comparing the intermediate or mega floor fire. In case of mega floor fire, the diagrid connection is not moment resistant. Due to the rotation allowed at the connection it has lesser restraint to the deformation. This can also be seen in the deflected shape in Fig. 25. The deflected shape in case of intermediate floor fire (a, b) is in the form a curve while there is a sharp kink in case of mega floor (c, d) fire which results in more outward displacement. Similarly, the inward deflection is also higher in mega floor fire.

The compressive axial forces develop in the fire floor due to the restraint provided by internal columns and the diagrid. Since there is relatively lesser restraint in case of mega floor fire, lower compressive forces develop in the floor. This can be seen in Fig. 40, where the sum of

axial forces of Beam 1-5 has been plotted for Bay 1. The total force exerted by the floor on diagrid is 20% higher in case of intermediate floor fire.

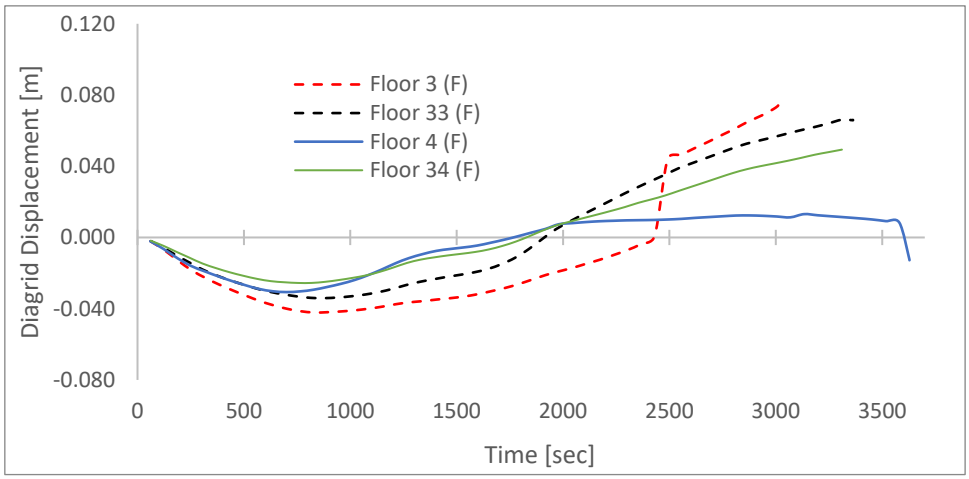

Fig. 39 Diagrid Lateral Displacement

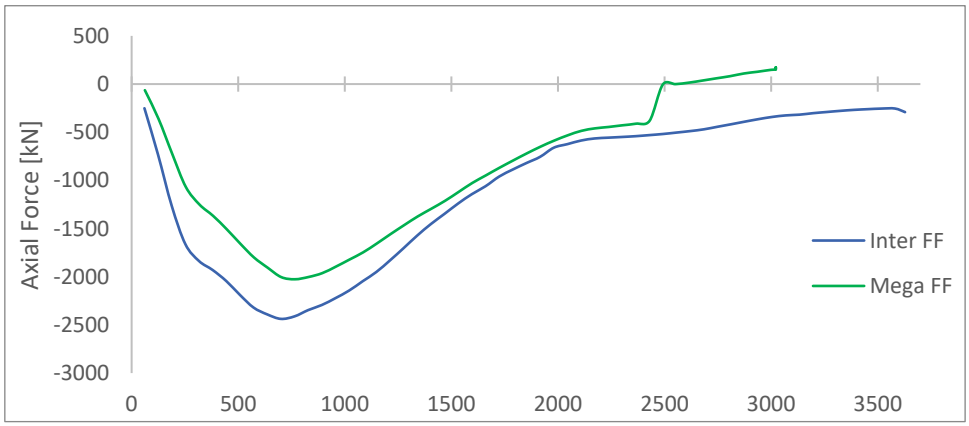

Fig. 40 Total Axial forces in the Fire Floor, Intermediate Floor fire and Mega Floor fire

Maximum tensile forces develop in floors adjacent to the fire floor. The comparison can be drawn for intermediate and Mega floor fires. Fig. 41 shows the axial forces in the floor above and below the fire floor. It can be seen that the axial forces are higher in case of an intermediate floor fire. The peak force is 40% higher for the floor above the fire floor and is 110% higher for the floor below.

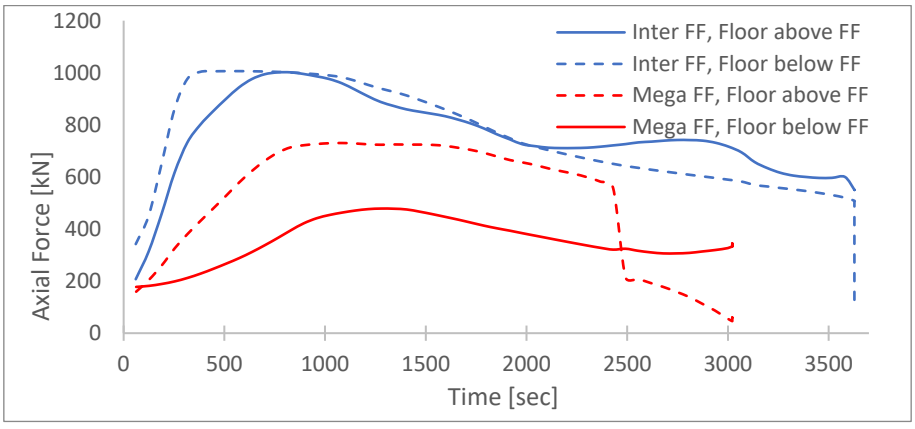

Fig. 41 Axial forces in Floor above and below fire floor

Moreover, the forces in the floor above and below the fire floor are almost equal in case of intermediate floor fire while in case of mega floor fire the forces are 53% higher than the floor below. The reason for this difference can also be explained by the connection of diagrid. As the connection is pushed outwards by the thermal expansion of the floor, extra moment is generated at the lower part of column at fire floor. This can be seen in the deflected shape of diagrids in Fig. 25 (a, c). The lower part of column is slightly bent inwards. There are high axial forces in the diagrid due to the load of upper structure. As the floor 3 moves outwards, an extra P-δ moment is generated which acts on the base of column, pushing it inwards. This moment is not significant in the intermediate floor fire because of lesser eccentricity due to lesser outward displacement of the diagrid.

Fig. 42 shows the deflection in fire floors for all fire scenarios. The data shows that maximum deflection is in case of mega floor fire in the strip model. This is also the pattern discussed in section 3.3. the outer floor beams on the edge (Beam 1 & 5) form a plastic hinge and slab deflects from 85 cm to 100 cm in 90 sec.

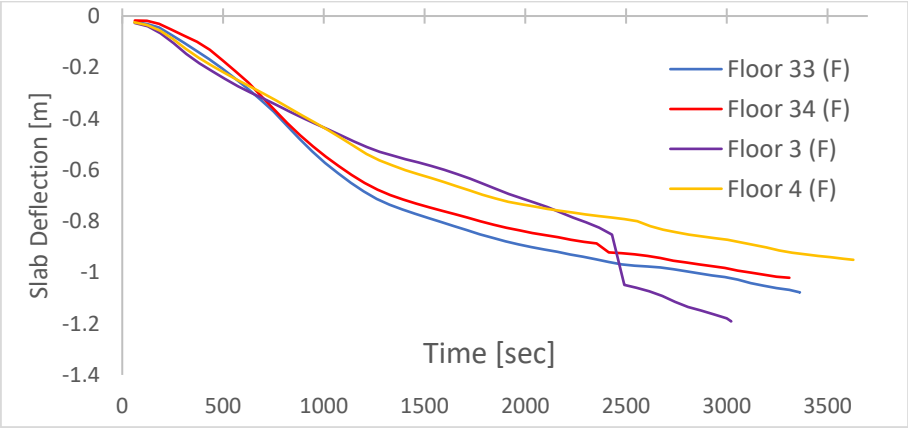

Fig. 42 Slab deflection, all fire floors

Fig. 43 shows the mid-span moment of each bay for both scenarios of strip model. The figure indicates that the highest moment is developed in the middle bay of both scenarios and the moment in all bays is higher for intermediate floor fire.

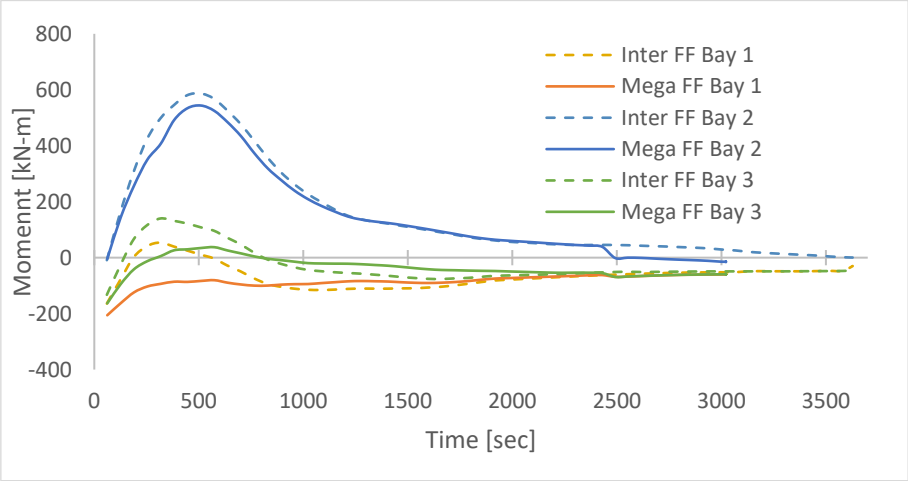

Fig. 43Mid-span moment in each bay, Intermediate and Mega Floor fire, Strip Model

The failure was identified when the convergence could not be achieved after the buckling of an element or the excessive deflection. In case of strip model of intermediate floor fire scenario, the output showed a local failure of diagrid buckling. There was no significant deformation observed in the internal columns. The maximum displacement for the columns was 4-5 mm. But it could be argued that when the load will be transferred to other structural members, a global failure could occur. Similarly, in case of mega floor fire where the plastic hinge formed in the beams, after some time the simulation showed that a deflection was too large and solution didn't converge. This was also a local failure of fire floor and no global response was captured.

4. Discussion

The general sequence of events is same in all the models. However, the magnitude of displacement, moment and stresses generated differs. Thermal expansion takes place in the fire floor which pushes the diagrid outwards. The diagrid experiences high axial and bending forces. As the heating continues, slab deflects due to the thermal gradient in the slab and axial compressive forces due to the end restraint. Fire floor experiences high compressive and flexural stresses.

The main findings can be summarized as follows:

- The axial compressive forces in fire floor and the axial tensile forces in the adjacent floors are higher in case of intermediate floor fire.
- The diagrid lateral displacement in both directions (outwards and inwards) is higher in case of mega floor fire. This displacement depends on the relative stiffness of the floor beams and diagrid section. Higher inward displacement of diagrid was seen in case of corner models where diagrid section is smaller.
- In case of mega floor fire, higher P-δ moment is generated at the base of diagrid in fire floor. While this is lesser in case of intermediate floor fire.
- In case of the fire on the lower floors, failure is initiated by the buckling of the diagrid at the base of fire floor in the intermediate floor fire. In case of mega floor fire, the failure is initiated by the plastic hinge formation in the floor beam.
- Catenary mechanism occurred in the floor bays adjacent to the diagrid. This mechanism was not observed in Bay 2 which was restrained on both sides by the internal columns.
- Deflection in the middle bay, Bay 2, occurred due to temperature gradient and thermal expansion. While in the side bays, Bay 1 & 3, the deflection increased due to the additional tensile strains due to the catenary action.

Though, no global failure was observed in the simulations but it can be assumed, that as the load will be transferred to other structural elements, it may lead to global failure soon.

The analysis was run considering TIMESTEPMIN of 2.0E-5 sec for the convergence. The convergence was not achieved after the buckling of 2,3 elements or if the deflection was too large. Due to the work stoppage, new simulations could not be run. But it is expected that if the minimum time step for convergence is reduced further, the simulation may run longer thereby showing the propagation of failure. Though, it can be argued that if the floors adjacent to the fire floor are stiff enough, and the internal columns, which didn't show any significant deformation, may stand longer but the probability of this is very low. Because in the standard fire curve, the temperature will rise further. Structural members will lose the strength and eventually the whole structure will lose its stability.

However, if the cooling phase is considered as in the case of parametric fire curve, there could be the possibility that global failure will not occur. Looking at the stability of structure after the plastic hinge formation in mega floor fire scenario, it can be expected that if temperature start to decrease at that stage, the structure may withstand after local failure.

The internal configuration of the building is very important in the performance of the diagrid structure. In this case, the size of internal columns was significantly large as compared to the diagrid section. This provides very high lateral strain to the beams in the middle bay of the building. So, if the free span of floor beams is longer, it will develop higher stresses in the diagrid.

The prescriptive fire protection does not guarantee the overall performance of the structure in case of fire. The results of this study also give the idea of critical locations of structural members where higher stresses are developed. This may help in the performance-based fire safety design of the diagrid building. The fire protection can be provided to the critical structural members rather than all members. This may save cost and also improve the overall performance of the structure.

5. Conclusion

In this study, response of tall building diagrid structure has been studied when subjected to standard fire curve, ISO-834. Two fire scenarios were considered: one for an intermediate floor fire and second for a mega floor fire. The results show that the overall response of the structure is similar in the initial stages for both scenarios. However, the magnitude of displacement, moment and stresses generated differs. The diagrid lateral displacement in both directions (outwards and inwards) is higher in case of mega floor fire. The fire floor experiences very high compressive stresses due to the restraint to thermal expansion by diagrid and internal columns. The floors adjacent to the fire floor experience the highest axial tensile forces. These tensile forces reduce as we move to the floors away from fire floor.

The total axial compressive force exerted by diagrid to the fire floor in case of intermediate floor fire is 20% higher than that of mega floor fire. The tensile axial forces are also higher in case of intermediate floor fire. Tensile forces in the upper floor are 40% higher and in case of lower floor 110% higher in intermediate floor fire than mega floor fire. Moreover, tensile forces are almost equal in upper and lower floor in intermediate floor fire. In mega floor fire these forces are 53% higher in upper floor than the lower floor.

The catenary mechanism is developed in Bay 1 & 3. Thus, mid span deflection is higher in these Bays than in Bay 2. In mega floor fire Bay 1 deflection is 119 cm and in Bay 2 is 81cm. in intermediate floor fire this deflection is 98 cm in Bay 1 and 90 cm in Bay 2.

No global failure was observed in any scenario. In case of fire on the lower floors, failure in intermediate floor fire was initiated by the buckling of diagrid due to high temperature and axial loads. While in mega floor fire failure occurred due to the formation of plastic hinge in the floor beams. In case of fire on upper floors, failure was identified as excessive deflections in the floor.

The scope of this work is limited to few scenarios which cannot reflect the overall response of structure to the fire. More work can be carried out by multiple scenarios and changing the stiffness of structural members for the same fire scenario.

The structural response of diagrid structure also depends on the geometry of the internal structure and the angle of inclination of diagrid members. More work can be carried out by studying these parameters and response of the structure to the fire. The connection types can also be varied for the diagrid nodes and beam column joint. Moreover, only standard fire has been applied in this study. The work can be extended to more realistic fire scenarios like parametric fire curve and travelling fires.

Acknowledgement

My efforts needed a direction and myself a motivation; I got these both from my thesis supervisor Dr. David Lange for which I would like to pay my deepest gratitude. He guided me throughout the project with incredible energy and coached me to improve my approach towards research. Besides his mentoring in academics, his unmatched support in this unusual stressful time due to COVID-19 is also equally acknowledged.

I would also like to thank my supervisor from The University of Edinburg Dr. Angus Law and my personal tutor Dr. Grunde Jomaas for always being there for the support.

I am grateful to my peers and family for their unwavering support and love during my study, especially my friend Muhammad Shafaat Nawaz. I would like to thank IMFSE management for organizing group Skype calls to stay updated and connected throughout this stressful time.

I genuinely believe that I would never have made it this far without support from all these beautiful people.

References

[1] T. Meyer Boake, *Diagrid Structures*. DE GRUYTER, 2014.

[2] M. R. Maqhareh, "The Evolutionary Process of Diagrid Structure Towards Architectural, Structural and Sustainability Concepts: Reviewing Case Studies," *J. Archit. Eng. Technol.*, vol. 03, no. 02, 2014, doi: 10.4172/2168-9717.1000121.

[3] K. Jani and P. V. Patel, "Analysis and design of diagrid structural system for high rise steel buildings," *Procedia Eng.*, vol. 51, pp. 92–100, 2013, doi: 10.1016/j.proeng.2013.01.015.

[4] M. M. Ali and K. S. Moon, "Structural Developments in Tall Buildings: Current Trends and Future Prospects," *Archit. Sci. Rev.*, vol. 50, no. 3, pp. 205–223, 2007, doi: 10.3763/asre.2007.5027.

[5] K. S. Moon, J. J. Connor, and J. E. Fernandez, "Diagrid structural systems for tall buildings: Characteristics and methodology for preliminary design," *Struct. Des. Tall Spec. Build.*, vol. 16, no. 2, pp. 205–230, 2007, doi: 10.1002/tal.311.

[6] "The Gherkin: How London's Famous Tower Leveraged Risk and Became an Icon | ArchDaily." https://www.archdaily.com/445413/the-gherkin-how-london-s-famous-tower-leveraged-risk-and-became-an-icon (accessed Apr. 29, 2020).

[7] "H E U R O P E A N N I O N," vol. 1, no. 2005, 2011.

[8] C. G. Bailey, "Fire engineering design of steel structures," *Adv. Struct. Eng.*, vol. 8, no. 3, pp. 185–202, 2005, doi: 10.1260/1369433054349141.

[9] A. S. Usmani, J. M. Rotter, S. Lamont, A. M. Sanad, and M. Gillie, "Fundamental principles of structural behaviour under thermal effects," *Fire Saf. J.*, vol. 36, no. 8, pp. 721–744, 2001, doi: 10.1016/S0379-7112(01)00037-6.

[10] A. Usmani, C. Roben, and A. Al-Remal, "A very simple method for assessing tall building safety in major fires," *Int. J. Steel Struct.*, vol. 9, no. 1, pp. 17–28, 2009, doi: 10.1007/bf03249476.

[11] D. Lange, C. Röben, and A. Usmani, "Tall building collapse mechanisms initiated by fire: Mechanisms and design methodology," *Eng. Struct.*, vol. 36, pp. 90–103, 2012, doi: 10.1016/j.engstruct.2011.10.003.

[12] P. Kotsovinos, A. Law, S. Deeny, and N. A. Butterworth, "Structural fire response of tall buidlings with inclined and bi-linear perimeter columns," 2014, pp. 1031–1038.

[13] A. Law, P. Kotsovinos, and N. Butterworth, "Engineering geometrically bi-linear columns to deliver fire resistance: Standard heating," *Eng. Struct.*, vol. 100, pp. 590–598, 2015, doi: 10.1016/j.engstruct.2015.06.046.

[14] F. Wald *et al.*, “Experimental behaviour of a steel structure under natural fire,” *Fire Saf. J.*, vol. 41, no. 7, pp. 509–522, 2006, doi: 10.1016/j.firesaf.2006.05.006.

[15] O. Vassart *et al.*, “Fire resistance of long span cellular beam made of rolled profiles (FICEB),” no. April, 2011.

[16] B. K.-U. K. B. S. S. Technology and undefined 1998, “The behaviour of a multi-storey steel framed building subject to fire attack–experimental data.”

[17] E. Rackauskaite, P. Kotsovinos, A. Jeffers, and G. Rein, “Computational analysis of thermal and structural failure criteria of a multi-storey steel frame exposed to fire,” *Eng. Struct.*, vol. 180, no. November 2018, pp. 524–543, 2019, doi: 10.1016/j.engstruct.2018.11.026.

[18] S. Engineering, “Manual of SAFIR - Mechanical,” no. January, 2019.

[19] T. Gernay, A. Millard, and J. M. Franssen, “A multiaxial constitutive model for concrete in the fire situation: Theoretical formulation,” *Int. J. Solids Struct.*, vol. 50, no. 22–23, pp. 3659–3673, Oct. 2013, doi: 10.1016/j.ijsolstr.2013.07.013.